JOURNAL OF GEOPHYSICAL RESEARCH, VOL. 113, D08212, doi:10.1029/2007JD009192, 2008

Submicron particles at Thompson Farm during ICARTT measured using aerosol mass spectrometry

Laura D. Cottrell,[1,2] Robert J. Griffin,[1,3] Jose L. Jimenez,[4] Qi Zhang,[5] Ingrid Ulbrich,[4] Luke D. Ziemba,[1] Pieter J. Beckman,[1] Barkley C. Sive,[1] and Robert W. Talbot[1]

Received 19 July 2007; revised 16 October 2007; accepted 18 December 2007; published 24 April 2008.

[1] The composition and size of aerosols were measured using an Aerodyne quadrupole aerosol mass spectrometer at Thompson Farm in Durham, NH, during the International Consortium for Atmospheric Research on Transport and Transformation campaign during summer 2004. Submicron, non-refractory aerosol was dominated by organic matter and sulfate (averages of 5.7 μg m^{-3} and 3.6 μg m^{-3}, respectively), with smaller contributions from nitrate and ammonium (averages of 0.3 μg m^{-3} and 1.02 μg m^{-3}, respectively). Organic aerosol (OA) mass correlates well with anthropogenic tracers such as carbon monoxide (CO, R^2 = 0.58) and black carbon (R^2 = 0.59), but multiple analyses indicate possible contributions from primary, secondary, anthropogenic, and biogenic OA. Multivariate statistical analysis of the OA mass spectra indicates the presence of two types of oxygenated OA (OOA) and a hydrocarbon-like OA (HOA) component that also contains contributions from biomass burning OA (BBOA). On average, the HOA/BBOA component accounts for 21% of the total OA mass while the two OOA components account for 24% and 55%, respectively, of the OA burden. Observed nitrate correlates well with OA (R^2 = 0.67), suggesting interference, the presence of organic nitrates, processing/uptake of nitric acid by OA, or other temporally coincident processes because of the ammonia-poor environment with respect to sulfate. The relative increase of OA with respect to background compared to that of CO (average of 72.7 μg m^{-3} ppmv^{-1}) indicates values that are higher than those based on previous measurements in New England.

Citation: Cottrell, L. D., R. J. Griffin, J. L. Jimenez, Q. Zhang, I. Ulbrich, L. D. Ziemba, P. J. Beckman, B. C. Sive, and R. W. Talbot (2008), Submicron particles at Thompson Farm during ICARTT measured using aerosol mass spectrometry, *J. Geophys. Res.*, *113*, D08212, doi:10.1029/2007JD009192.

1. Introduction

[2] Particulate matter (PM), or aerosol, is an important trace constituent of the atmosphere. In the troposphere, these particles play an important role in human health in that increased levels of PM have been correlated statistically to increased human morbidity and mortality [*Pope et al.*, 2002]. Despite efforts to reduce the emission of primary aerosols and of precursors to secondary aerosols, many areas still do not comply with established air quality standards for PM [*United States Environmental Protection Agency*, 2001]. Climate is affected directly (through scattering/absorption of solar short-wave radiation and/or planetary long-wave radiation) and indirectly (effects on cloud droplet size, number concentration, and lifetime) by aerosols [*Intergovernmental Panel on Climate Change*, 2001]. Particles also contribute to haze associated with pollution due to their ability to cause light extinction [*Schichtel et al.*, 2005].

[3] The International Consortium for Atmospheric Research on Transport and Transformation (ICARTT) campaign was designed to study the formation, processing, and transport of aerosols, ozone (O_3), and their precursors over the northeastern United States, the North Atlantic Ocean, and Europe from 1 July through 15 August 2004 [*Fehsenfeld et al.*, 2006]. Several ground stations and aircraft as well as the National Oceanic and Atmospheric Administration (NOAA) Research Vessel (RV) *Ronald H. Brown* were used as platforms for measuring a suite of atmospheric constituents and meteorological parameters. The University of New Hampshire (UNH) Atmospheric Observatory at Thompson Farm in Durham, NH (henceforth referred to simply as Thompson Farm), served as one of the ground stations during the campaign. Since late 2001, this monitoring station has operated year-round as part of the AIRMAP Cooperative Institute established by UNH and NOAA.

[4] Thompson Farm is located in a semi-rural environment in southeastern New Hampshire (43.11°N, 70.95°W,

[1]Climate Change Research Center, University of New Hampshire, Durham, New Hampshire, USA.
[2]Currently at Environ, Groton, Massachusetts, USA.
[3]Also at Department of Earth Sciences, University of New Hampshire, Durham, New Hampshire, USA.
[4]Department of Chemistry and Biochemistry and Cooperative Institute for Research in the Environmental Sciences (CIRES), University of Colorado, Boulder, Colorado, USA.
[5]Atmospheric Sciences Research Center, State University of New York, University at Albany, Albany, New York, USA.

0148-0227/08/2007JD009192$09.00

24 m above sea level), 20 km west of the Gulf of Maine and 100 km north of Boston, MA. Because of the location of Thompson Farm, local point sources of anthropogenic aerosol and its precursors are relatively small, though automobile use on area highways is likely a regional area source. Large plumes of aerosol and other primary and photochemical pollutants are transported to rural New England from regions such as the Ohio River Valley and the east coast of the United States [*Fischer et al.*, 2004, 2007; *Ziemba et al.*, 2007]. In addition, Thompson Farm is subject to the influence of biogenic volatile organic compounds (VOCs) due to its location [*Griffin et al.*, 2004; *White et al.*, 2008]. The influences of coastal and oceanic areas [*Zhou et al.*, 2005, 2008] and of Canadian regions [*Mao and Talbot*, 2004] on trace species in the atmosphere at Thompson Farm also have been identified. The location of Thompson Farm clearly makes it an ideal site at which to study how different air mass types exert control on surface-level air quality.

[5] Aerosol concentration data collected using an Aerodyne (Billerica, MA) quadrupole aerosol mass spectrometer (Q-AMS) deployed at Thompson Farm during ICARTT are reported here. These results provide a high resolution time series of the chemical composition and size distribution of submicron, non-refractory aerosol. This time series is analyzed in conjunction with additional aerosol, gas, and meteorological data. In addition to presenting collected data, this manuscript evaluates the importance of secondary organic aerosol (SOA) and considers its potential precursors and formation pathways through spectral and statistical analyses and the relationship between organic aerosol (OA) and carbon monoxide (CO). The data presented here are also compared to those collected on other ICARTT platforms and during the New England Air Quality Study (NEAQS) of 2002.

[6] It is expected that primary anthropogenic, secondary anthropogenic, and secondary biogenic OA will be observed at this location in the submicron size fraction. As will be discussed subsequently, biomass burning events also affected OA levels at Thompson Farm during ICARTT. Recent evidence suggests the presence of cellular material in a significant fraction of submicron atmospheric aerosols [*O'Dowd et al.*, 2004; *Jaenicke*, 2005]. It is assumed that the primary biogenic component at Thompson Farm is small because the mechanical generation processes required for most of this type of material to be emitted to the atmosphere from plants [*Seinfeld and Pandis*, 2006] would tend to produce particles at the upper end of the submicron mode (which is sampled less efficiently by the Q-AMS). The relatively small influence of marine sectors on aerosols at this location [*Ziemba et al.*, 2007] also supports the assumption of a small impact from submicron primary OA (POA) from a marine source, such as that described by *O'Dowd et al.* [2004].

[7] *deGouw et al.* [2005] and *Marcolli et al.* [2006] concluded that OA off the coast of New England during NEAQS likely was dominated by anthropogenic SOA, a conclusion echoed by *Quinn et al.* [2006] for ICARTT. This idea is supported by the results of *Sullivan et al.* [2006] whose airborne measurements of water-soluble particulate organic carbon (WSPOC) during ICARTT in the lowest two kilometers of the troposphere showed relatively high concentrations in urban plumes but relatively low ones in rural areas. In contrast, the study of *White et al.* [2008] showed that monoterpenes and isoprene contributed very strongly to hydrocarbon reactivity at Thompson Farm during ICARTT. In addition, using best estimates of precursor emissions and meteorology, *Chen et al.* [2006] simulated SOA formation in the area surrounding Thompson Farm for 3–4 August 2004, and found that the dominant contributor to simulated SOA formation was oxidation of monoterpenes. However, recent work by *Volkamer et al.* [2006] indicates that anthropogenic SOA likely is underpredicted by a factor of eight in current models. Therefore this study was pursued because the chemical and physical processes that control OA levels at Thompson Farm remain unclear.

2. Instruments and Methods

2.1. Aerodyne Q-AMS

[8] The Q-AMS is described in great detail elsewhere [*Jayne et al.*, 2000; *Jimenez et al.*, 2003]; therefore, only a brief description is given here. Aerosol enters the instrument through a 130-μm critical orifice, and aerosol particles are focused into a narrow beam using an aerodynamic focusing lens [*Liu et al.*, 1995a, 1995b]. While most of the gas is pumped away, the particle beam travels across a vacuum chamber, at the end of which particles are vaporized on a resistively heated surface and ionized under a 70-eV electron impact (EI) ionization source. The ions are filtered by their mass-to-charge (m/z) ratio in a Balzers (Balzers, Lichtenstein) QMA 410 quadrupole mass spectrometer and detected with a secondary electron multiplier.

[9] The Q-AMS measured the chemical composition and size distribution of submicron, non-refractory aerosol in ten-minute intervals during the campaign. This measurement is referred to as submicron in the sense of the standard PM_1 definition because, as is the case for other PM_1 instruments that use cyclones to make the size cut, the lens on the Q-AMS actually does not transmit all submicron particles with complete efficiency. The actual window of 100% transmission through the lens is roughly 60–600 nm, with transmission efficiency decreasing rapidly beyond these limits [*Liu et al.*, 1995a, 1995b; *Jayne et al.*, 2000]. Corrections are not made to account for this transmission efficiency [*Allan et al.*, 2003]. For total mass, these issues likely are minimized by data corrections discussed subsequently. When actual size distributions include small contributions from particles larger than 600 nm in diameter [*Brock et al.*, 2008], typically in urban and biomass burning plumes, the size distributions shown in this work will be skewed artificially to sizes smaller than 600 nm. The term non-refractory refers to material that will vaporize rapidly at the temperature of the heater in the Q-AMS, which was maintained at 550°C during this campaign, precluding detection of soil dust, metal, black carbon (BC), and sea salt.

[10] The Q-AMS operated in two modes throughout the campaign: mass spectrum (MS) and particle time-of-flight (PToF). While in the MS mode, the Q-AMS scanned the entire spectrum from 1 to 330 atomic mass units (amu) at 1 amu ms^{-1} with a resolution of 1 amu, thereby providing mass loading information for all fragment ions less than 331 amu. Size information was obtained in the PToF mode, during which the vacuum aerodynamic diameter (D_{va}) of

particles was calculated based on the traveltime in the vacuum chamber [*DeCarlo et al.*, 2004].

[11] Mass/ionization efficiency calibrations of the Q-AMS were performed on-site every two to three days during the campaign using monodisperse (selected using a differential mobility analyzer) ammonium nitrate aerosol generated with an atomized solution and dried in a diffusion dryer. Instrument response was assumed to be linear for all concentrations [*Jayne et al.*, 2000], and the relative ionization efficiency of each compound was based on previous laboratory experiments [*Alfarra et al.*, 2004]. Size calibrations were performed using National Institute of Standards-traceable polystyrene latex spheres before and after the campaign.

[12] All organic mass loadings were corrected for interference from the atmospheric carbon dioxide (CO_2) signal using additional AIRMAP CO_2 data that are not shown here. All mass loadings were corrected for reduced particle collection efficiency (CE), presumably due to particle bounce [*Drewnick et al.*, 2003; *Hogrefe et al.*, 2004; *Huffman et al.*, 2005; *Takami et al.*, 2005; *Zhang et al.*, 2005a]. Collection efficiency is influenced by factors such as relative humidity, acidity, and particle composition [*Kleinman et al.*, 2005; *Rhupaketi et al.*, 2005; *Zhang et al.*, 2005a, 2005b; B. M. Matthew, T. B. Onasch, and A. M. Middlebrook, Collection efficiencies in an Aerodyne aerosol mass spectrometer as a function of particle phase for laboratory generated aerosols, submitted to *Aerosol Science and Technology*, 2008; *Salcedo et al.*, 2007], but a definitive quantitative relationship between the CE and the factors on which it depends has yet to be determined. Therefore a CE of 0.5 was used for all mass loadings in this study based on comparison to the sulfate fraction of concurrent filter measurements of $PM_{2.5}$ (R^2 = 0.77) [*Ziemba et al.*, 2007]. The CE due to particle bounce is one of the largest sources of uncertainty in these measurements. All data were processed and evaluated using the algorithms described by *Jimenez et al.* [2003] and *Allan et al.* [2003, 2004]. For this study (ten-minute averages), the lower detection limits of the Q-AMS were 0.06 μg m^{-3}, 0.14 μg m^{-3}, 0.01 μg m^{-3}, and 0.19 μg m^{-3} for sulfate, ammonium, nitrate, and organic material, respectively. Corroborating particle composition data of high temporal resolution were not available for this location during ICARTT; therefore, an uncertainty of ±40% is applicable to the data presented here.

[13] The Q-AMS was located in a trailer adjacent to the 15-m, instrumented, walk-up tower from which it sampled. Sample was drawn from the top of the tower through a 0.5-inch outer diameter (OD) length of copper tubing with a University Research Glass (Chapel Hill, NC) 2.5-μm cyclone on the inlet. The cyclone removes only particles larger than a micron in diameter; therefore, it is assumed that the presence of the cyclone did not affect the mass concentrations measured by the Q-AMS, as particles larger than a micron mostly are not transmitted through the aerodynamic focusing lens. This hypothesis was tested by removing the cyclone and observing no change in measured mass loadings. A constant laminar flow of 10 L min^{-1} was maintained by pumping through a critical orifice downstream of the Q-AMS. The Q-AMS sub-sampled isokinetically from the inlet line at approximately 150 mL min^{-1}.

2.2. Additional Measurements

[14] Additional relevant measurements discussed here include concentrations/mixing ratios of particle number, BC, CO, sulfur dioxide (SO_2), nitric oxide and nitrogen dioxide (NO and NO_2), and select VOCs, both hydrocarbons and oxygenates. The instruments used for these measurements, respectively, were a TSI (St. Paul, MN) 3022 condensation particle counter, a Magee Scientific (Berkeley, CA) AE31 aethalometer, a Thermo Environmental Instruments (TEI) (Waltham, MA) model 48C CO analyzer, a TEI model 43C SO_2 analyzer, a high-resolution custom-built monitor for NO and NO_2 [*Griffin et al.*, 2007], an automated four-channel gas-chromatograph (GC) equipped with two flame ionization detectors (FID) and two electron capture detectors [*Sive et al.*, 2005; *Zhou et al.*, 2005, 2008], and an Ionicon Analytik (Innsbruck, Austria) Proton Transfer Reaction Mass Spectrometer (PTR-MS). Additional details of VOC calibration, collection, and analysis are provided by *Talbot et al.* [2005] and *White et al.* [2008]. GC-FID was also used to measure methane. These instruments were located in a building at the base of the tower from which the Q-AMS sampled. These instruments sub-sampled from a 10.2-cm OD Teflon®-coated aluminum manifold that carried air from the top of the tower at 1000 L min^{-1}.

2.3. Backward Trajectories

[15] In an effort to classify in general terms the source regions affecting the sampled aerosol material, the HYbrid Single Particle Lagrangian Integrated Trajectory (HYSPLIT) model [*Draxler and Rolph*, 2003] was used. In accordance with the techniques described by *Ziemba et al.* [2007], three seventy-two hour backward trajectories were computed for each calendar day at 1200, 2000, and 0400 local time. Trajectories were initialized at a height of 750 m above mean sea level; meteorological inputs for the trajectory calculations were taken from the Eta Data Assimilation System grid.

[16] The trajectories for each day and time were classified into one of the six source regions described by *Ziemba et al.* [2007]: Continental-Midwest (CMW), Continental-Coastal (CC), Marine-Coastal (MC), Marine (MAR), Marine-Canada (MACA), and Continental-Canada (COCA). For further simplification in this manuscript, the CMW, CC, and MC regions are grouped together as the areas most likely influenced by anthropogenic activity, while the MAR, MACA, and COCA regions are grouped together as the areas most likely representative of background conditions. The period discussed below that was influenced most strongly by biomass burning is removed from this analysis and noted as such at the relevant places in the text.

3. Results

3.1. General Trends

[17] The aerosol measured at Thompson Farm during ICARTT consisted mostly of organic material and sulfate, with smaller contributions from ammonium and nitrate. As shown in Figures 1a–1d, the size distribution usually exhibited a prominent mode at a D_{va} of approximately 400 nm and, less frequently, a smaller mode at a D_{va} of approximately 150 nm, consisting most probably of fresh

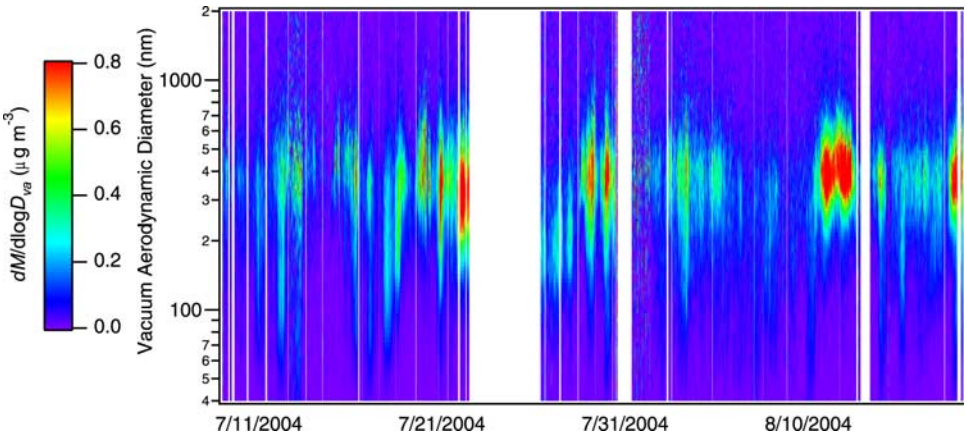

Figure 1a. Mass-based size (nm) distribution (μg m^{-3}) of aerosol nitrate at Thompson Farm during ICARTT.

POA based on size and dominant *m/z* signals present. Periods of high mass loading (Figure 1e) were dominated either by organic material alone (for example, the period of 11–13 July 2004) or by organic material and sulfate concurrently (for example, 11–13 August 2004). Ammonium, although present to a smaller degree, generally tracked sulfate; contributions of nitrate aerosol were small but tracked OA mass. Although not discernable due to the scale of the mass-based size distributions indicated in Figures 1a–1d, Thompson Farm also experienced in situ growth (for example, 7 August 2004), as indicated by the gradual increase of D_{va} as a function of time, as well as transport of large pollution plumes (for example, 11–13 August 2004), as indicated by the sudden appearance of large concentrations of aerosol species in the larger (400 nm) size fraction.

3.2. Sulfate

[18] The average mass loading of sulfate during the campaign was 3.6 ± 5.1 (one standard deviation, SD) μg m^{-3}, representing on average 33.9% of the observed aerosol mass. The median sulfate concentration was 1.6 μg m^{-3}, with the range of observed concentrations being 0.06 to 28.1 μg m^{-3}. The ratio between the average and the median is approximately 2.2, indicating the strong influence of large pollution events from the southwestern wind sector. On the basis of the medians of the hourly average concentrations over the entire campaign, it appears that sulfate aerosol did not exhibit a strong diurnal profile, with means and 95th percentile values exhibiting more hourly dependence.

[19] Sulfur dioxide may be converted to sulfate aerosol via in-cloud processing or via gas-phase oxidation by the hydroxyl radical (OH), though the latter process is relatively slow. Therefore local, less-processed plumes should have a higher mixing ratio of SO_2 relative to aerosol sulfate loading [*Fugas and Gentilizza*, 1978] assuming that there has been no favorable wet deposition of sulfate aerosol compared to SO_2 because of the relatively higher solubility of sulfate aerosol compared to SO_2 [*Brock et al.*, 2004]. During ICARTT, there were several examples at Thompson Farm of aerosol that appeared to be less processed with respect to sulfur, in contrast to the general ICARTT trend. Sharp increases in SO_2 and particle number concentration often occurred simultaneously, suggesting co-located local sources for SO_2 and particles (or potential new particle formation). Sulfate aerosol concentration data indicated coincident increases with SO_2 mixing ratio and particle number concentration in some instances as well, likely indicating local processing. This sulfate profile underscores the influence of both local and distal sources on air quality at Thompson Farm.

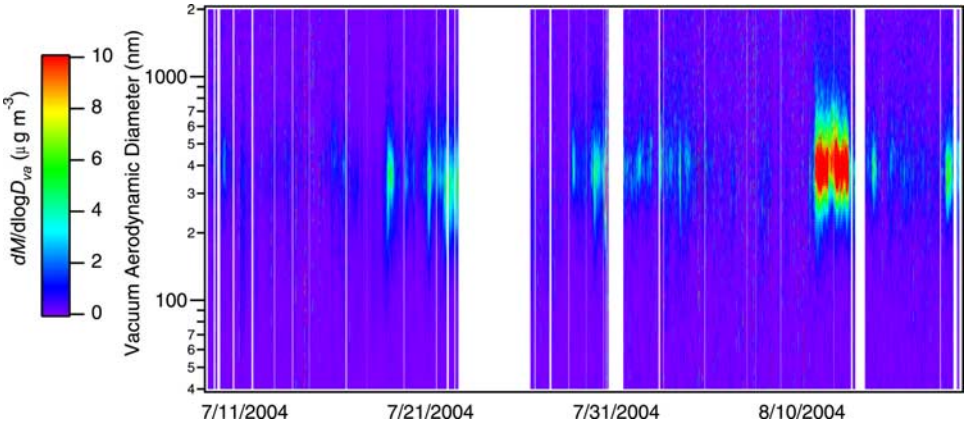

Figure 1b. Mass-based size (nm) distribution (μg m^{-3}) of aerosol ammonium at Thompson Farm during ICARTT.

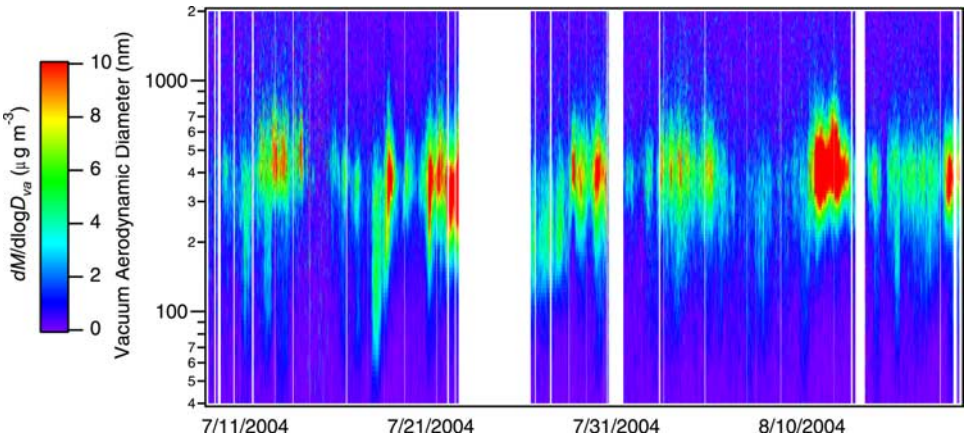

Figure 1c. Mass-based size (nm) distribution (μg m^{-3}) of aerosol organic material at Thompson Farm during ICARTT.

3.3. Ammonium

[20] Over the course of the campaign, the average observed ammonium concentration was 1.02 ± 1.35 (SD) μg m^{-3}, representing on average 9.6% of the observed aerosol mass. The median ammonium mass concentration was 0.54 μg m^{-3}, and the maximum observed concentration was 9.9 μg m^{-3}. Given that the average value is 1.9 times larger than the median (close to, but slightly smaller than, the factor of 2.2 for sulfate), it is again clear that Thompson Farm was affected strongly by large pollution events, generally from the southwest.

[21] Significant amounts of ammonium nitrate will not form easily in a relatively sulfate-rich, ammonia-poor environment such as that typical in the northeastern United States in summer [*Fischer et al.*, 2007]. Therefore ammonium mass loadings measured by the Q-AMS closely tracked sulfate during the entire campaign. A regression (Figure 2) of the molar concentrations of ammonium aerosol (x-variable) and sulfate aerosol (y-variable) indicates a slope of 0.7 (Ammonium bisulfate would have a slope of 1.0, and ammonium sulfate would have a slope of 0.5.) and a R^2 of 0.92. Ammonium sulfate would imply complete neutralization; therefore, this regression indicates a degree of acidity in the Q-AMS-sampled aerosols at Thompson Farm. In comparison, Q-AMS-sampled aerosols in Pittsburgh, PA, during the Pittsburgh Air Quality Study (PAQS) exhibited a slope of approximately 0.75 [*Zhang et al.*, 2005a, 2007a], while aerosols sampled with a Q-AMS at Chebogue Point, Nova Scotia, during ICARTT exhibited a slope of approximately 1.0 (J. D. Allan et al., Overview of in situ measurements of particle composition at Chebogue Point, Nova Scotia, during summer 2004 and insights into organic chemical processes, manuscript in preparation, 2008). This indicates aerosols measured at Thompson Farm during ICARTT were similarly neutralized as those measured during PAQS and less acidic than those measured at Chebogue Point.

3.4. Organic Material

[22] Organic material accounted for the majority of the total measured aerosol mass, with an average mass loading of 5.7 ± 3.6 (SD) μg m^{-3}, which accounted for an average of 53.7% of the observed aerosol mass. The median observation was 4.9 μg m^{-3}, and the range of measured values was 0.3 to 19.7 μg m^{-3}. In contrast to sulfate and ammonium, the ratio of the average to the median is less than 1.2 for OA concentration, indicating less influence of large pollution events compared to ammonium and sulfate. That is, OA appears to have had consistent source strengths in multiple upwind directions. As with sulfate, total mass loadings of organic material also showed a relatively flat diurnal pattern. Smaller organic particles, however, showed

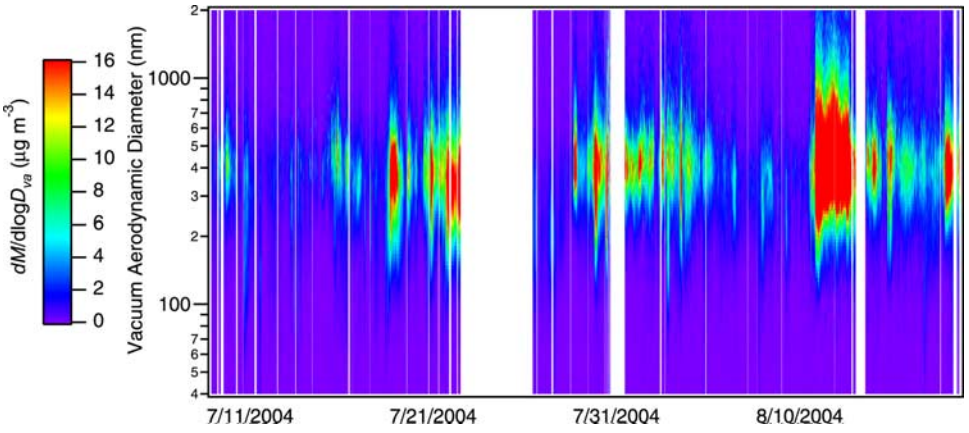

Figure 1d. Mass-based size (nm) distribution (μg m^{-3}) of aerosol sulfate at Thompson Farm during ICARTT.

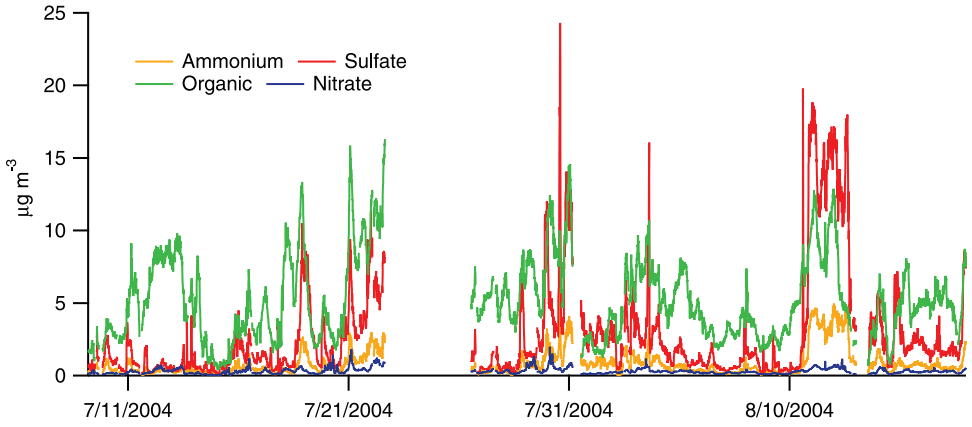

Figure 1e. Q-AMS-measured mass loadings (μg m^{-3}) of aerosol organic material, sulfate, nitrate, and ammonium at Thompson Farm during ICARTT.

a pronounced diurnal trend with a nighttime enhancement, probably resulting from a decreasing boundary layer height combined with carryover of daytime SOA concentrations and continued local emission of small combustion-related POA, as indicated by a relatively more intense presence of *m/z* 57 in the OA spectra [*Zhang et al.*, 2005c].

3.5. Nitrate

[23] As stated previously, nitrate aerosol concentrations in New England are expected to be relatively small during summer because this region generally tends to have large sulfate concentrations that interact preferentially with the ammonia that would be needed to form ammonium nitrate [*Fischer et al.*, 2007; *Ziemba et al.*, 2007]. It also appears that inorganic aerosol at this site is not neutralized completely. Therefore as expected, nitrate concentrations at Thompson Farm were relatively small during the course of the campaign. The average nitrate concentration was 0.3 μg m^{-3}, making up on average only 2.8% of the total non-refractory PM_1 mass. These values generally tracked but were slightly larger than small detectable nitrate concentrations in $PM_{2.5}$ sampled using filters and quantified using ion chromatography [*Ziemba et al.*, 2007].

[24] The ratio of the signals from the Q-AMS mass spectra for the two largest nitrate fragments, NO^+ (*m/z* 30) and NO_2^+ (*m/z* 46), estimated using the method of *Allan et al.* [2004], helps determine the chemical form of the sampled nitrate because various forms of nitrate fragment differently under EI ionization. For ammonium nitrate, the ratio of the signal at *m/z* 46 to that at *m/z* 30 is approximately one to two (1:1.8 for the Q-AMS used in this study, based on instrument calibrations), while the ratio for other forms of nitrate deviates from this value [*Bahreini et al.*, 2005; *Alfarra et al.*, 2006]. For laboratory experiments with other inorganic nitrates, this is due unequivocally to enhanced NO^+ relative to NO_2^+, while for organic nitrates this may also be due to enhancement of an organic fragment such as CH_2O^+ or CH_4N^+. When analyzing ambient data and applying the default assumptions of *Allan et al.* [2004], as done here, which estimate the organic contribution to *m/z* 30 as the ^{13}C isotopic fraction of the organic signal at *m/z* 29, it is also possible that some signal at *m/z* 30 from organic species other than organic nitrates is classified as nitrate [*Bae et al.*, 2007]. Future studies with the high-resolution version of the AMS [*DeCarlo et al.*, 2006] are likely to provide further insight into the contribution of various fragments to the signal at *m/z* 30.

[25] During ICARTT, the ratio of the signal at *m/z* 46 to that at *m/z* 30 in the ambient aerosol was approximately one to four based on the slope of a scatterplot between the two (not shown). Because the organic fragmentation patterns observed here do not differ significantly from those observed during other ambient Q-AMS studies [*Alfarra et al.*, 2004; *Zhang et al.*, 2005a, 2005b, 2005c], this one to four ratio indicates that the nitrate likely is in another form, such as mineral, sea-salt, or organic nitrate. Again, it is also possible that oxygenated organics contribute to the signal at *m/z* 30 [*Bae et al.*, 2007].

[26] It is unlikely that significant contributions of mineral nitrate would be present in the size range measured by the Q-AMS because the influence of fine soil material is thought to be negligible based on very small concentrations of Ca^{2+} on concurrent $PM_{2.5}$ filter samples [*Ziemba et al.*, 2007]. It is possible that nitrate associated with this size mode is sampled at Thompson Farm as a result of nitrate displacement of chloride in small particles of sea salt [*Gard*

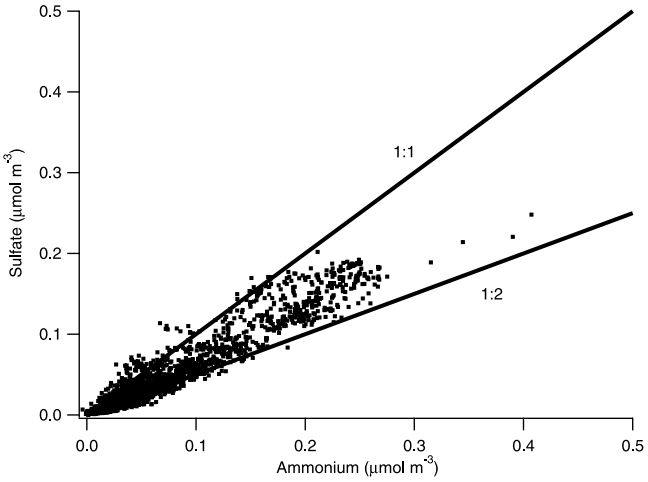

Figure 2. A regression between molar aerosol concentrations (μmol m^{-3}) of ammonium and sulfate measured at Thompson Farm during ICARTT.

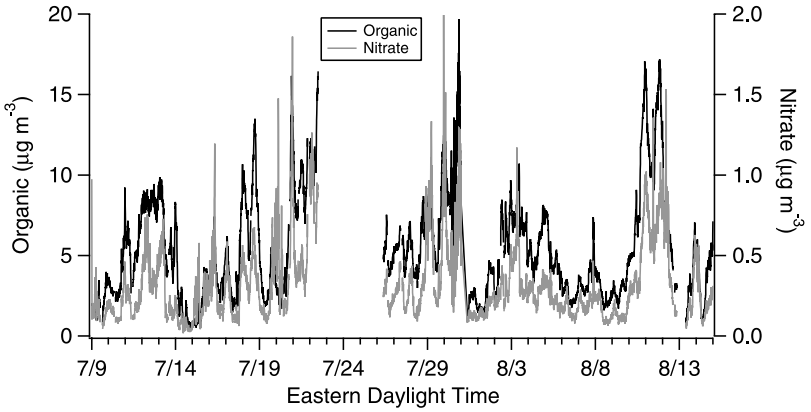

Figure 3. Mass loadings of Q-AMS-measured nitrate and OA (μg m^{-3}) over the course of ICARTT at Thompson Farm.

et al., 1998], though little influence of marine aerosol is likely to be experienced at Thompson Farm because of prevailing wind patterns [*Ziemba et al.*, 2007].

[27] The nitrate aerosol mass loading closely tracked that of OA mass, as shown in Figure 3; a regression between the two yields a R^2 of 0.67. This suggests that at least some portion of the nitrate is in the form of organic nitrate, possibly that OA provides surface area for heterogeneous uptake (either via reaction or physical sorption) of nitric acid, as suggested by *Jacob* [2000], or there is an interference of OA in the *m/z* 30 signal [*Bae et al.*, 2007]. Nitrate and OA also could be correlated because of separate processes occurring at the same time. For example, at night, OA may increase slightly due to a decrease in the boundary layer height while POA emissions continue. Heterogeneous hydrolysis of dinitrogen pentoxide may contribute to increased nitrate aerosol at night as well [*Brown et al.*, 2006]. Figure 4 shows a plot of molar nitrate concentration versus the molar ratio of ammonium to sulfate. Traditional thermodynamics would indicate that significant nitrate aerosol would not form unless the ammonium to sulfate ratio were greater than 2.0. Figure 4 clearly shows that nitrate formation occurs even at times when this ratio is less than 2.0, indicating that other factors contribute to mass attributed to nitrate at Thompson Farm.

[28] Figure 4 also is shaded by local hour of the day to investigate the temporal behavior of this relationship. While nighttime hours associated with lower temperatures and higher relative humidities (red and dark blue) are associated with all levels of nitrate aerosol, daytime hours (green) tend to be associated with lower values of nitrate. Size distribution data of Q-AMS-measured nitrate indicated that it was found primarily in the accumulation mode; therefore, it is likely that if nitrate is forming heterogeneously at night, it is doing so on larger particles containing a mixture of sulfate, ammonium, and organics as opposed to small combustion-related POA.

4. Discussion

4.1. OA/BC Technique

[29] The ratio of the concentrations of OA and BC may be used as an indicator of the formation of SOA [*Turpin and Huntzicker*, 1991]. This method assumes that there is a characteristic regional emission ratio of POA to BC, which is purely primary. Any increases in the ratio of OA to BC compared to the characteristic value are attributed to SOA formation. This method needs to be applied with caution because the POA to BC emissions ratio varies under different combustion conditions [*Shah et al.*, 2004]. In addition, at different times of the day and on different days of the week, changes in BC emissions influence changes in the ratio to a much greater extent than do changes in OA [*Harley et al.*, 2005]. It should also be noted that BC and OA are likely to have different removal mechanisms in the atmosphere, also adding uncertainty to the results derived from this method.

[30] For application to the ICARTT data set, BC concentrations from the aethalometer were averaged to 10 min in order to match the temporal resolution of the Q-AMS. Ratios were calculated only when both measurements were available. The fraction of OA that was primary (f_p) and that which was secondary (f_s) were estimated by comparing the observed ratio of OA to BC concentrations ((OA/BC)$_{obs}$) to a regional emissions ratio, E:

$$f_p = \frac{E}{(\mathrm{OA/BC})_{obs}} \tag{1a}$$

$$f_s = 1 - f_p \tag{1b}$$

Using a typical value of E of approximately 1.7 from tunnel study values corrected for non-carbon contributions to POA mass [*Turpin and Lim*, 2001; *Zhang et al.*, 2005b], f_p for the ICARTT data set ranged from 0 to 93%, with an average of 13 ± 7% (SD), a value very similar to that observed by *deGouw et al.* [2005] during the summer of 2002 during NEAQS. Because this method focuses exclusively on total OA, it is not possible to attribute estimated SOA levels to either anthropogenic or biogenic precursors. Therefore for the remainder of this paper, the OA/BC method shown here will be used simply as a benchmark to show that the bulk of OA was likely secondary in nature at Thompson Farm during the summer months of ICARTT.

[31] This analysis includes 11–13 July 2004, a period influenced strongly by biomass burning [*Warneke et al.*, 2006; *Duck et al.*, 2007]. For biomass burning, the observed ratios of emitted organic carbon (OC) to BC are in the range

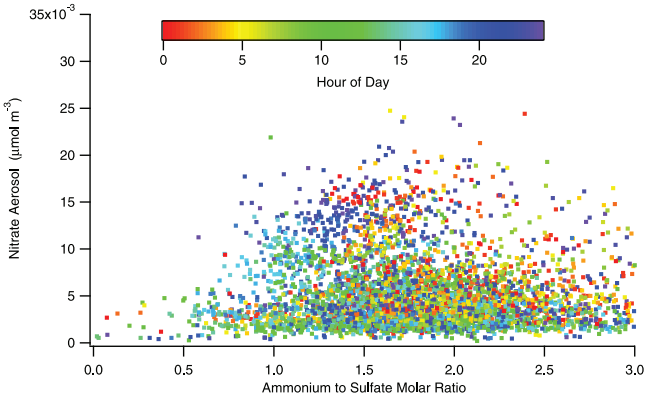

Figure 4. Molar aerosol nitrate concentrations (μmol m^{-3}) versus the molar aerosol ratio of ammonium to sulfate shaded by local hour of day during ICARTT. Higher values of the ammonium to sulfate ratio were observed during the campaign, but these values are not shown because they were associated with the lowest measured aerosol concentrations.

of 1.7 to 33.3 [*Reid et al.*, 2005]; these values are clearly significantly larger than the value assumed to represent POA at Thompson Farm for OA/BC. Very significant biomass burning influence was confined to only three days of the campaign based on PTR-MS measurements of acetonitrile [*Holzinger et al.*, 1999]. If these dates are removed from the analysis, very little change in the average predicted f_p values results. If the assumed weighted average E for Thompson Farm during ICARTT is doubled to 3.4 to account for biomass burning influence, the linearity of equation (1) results in an increase of the average f_p to 26%. Therefore it is estimated that the average f_p at Thompson Farm during ICARTT was likely in the range of 13 to 26%, with corresponding f_s values between 74 and 87%.

4.2. Bulk OA Spectral Analysis

[32] The average OA mass spectrum, expressed as the average percentage contribution of each *m/z* value to the total organic signal, for the entire campaign lends insight into the nature of the OA sampled at Thompson Farm during ICARTT, as shown in Figure 5. Note that this figure experiences essentially no change when biomass burning periods are removed. In addition, the average spectrum for the biomass burning periods is almost identical to that presented in Figure 5, suggesting that aged OA of different types result in similar spectra in the Q-AMS or that the fractional impact of biomass burning to OA during that period was not large.

[33] A method by which such average spectra from different campaigns can be compared is through regression between the percent contributions of specific *m/z* values. This is done for the ICARTT data in Figure 5 (x-variable) with the same information for total oxygenated OA (OOA) from PAQS [*Zhang et al.*, 2005c] and aged rural OA from the Lower Fraser Valley (LFV) in Canada [*Alfarra et al.*, 2004]. Only *m/z* values greater than 45 are considered in order to remove influence of smaller *m/z* values that dominate the signal; regressions are forced through zero. The stronger relationship results from the regression of Thompson Farm OA against aged rural OA from the LFV, which has a slope of 1.05 and an R^2 of 0.95, indicating that aged aerosol tends to have very similar Q-AMS spectra but giving no indication as to the source. In addition, the signal for the *m/z* values greater than 45 represented 36% of the total organic signal in each case. The regression between PAQS OOA and Thompson Farm OA was also significant ($R^2 = 0.89$) with a slope of 0.68. The change in slope likely results because only 23% of the total organic signal from the PAQS OOA spectrum is represented by the *m/z* values greater than 45.

[34] Additional insight into the nature of the sampled OA can be obtained through an ion series (or "delta") analysis of the mass spectra [*McLafferty and Turecek*, 1993; *Drewnick et al.*, 2004; *Schneider et al.*, 2004; *Bahreini et al.*, 2005]. In such an analysis, a delta value (Δ) is assigned to each *m/z* ratio based on the nominal number of carbons in the ion fragment. The relative intensity of the spectra for each Δ ($-7 \leq \Delta \leq 6$) indicates the likely type of molecules being analyzed by the Q-AMS. For example, $\Delta = 2$ indicates alkyl groups and saturated carbonyls (indicating both SOA and POA species), and $\Delta = 0$ indicates unsaturated species, predominantly hydrocarbons (indicating primarily POA species). The value $\Delta = 3$ indicates oxygenated organics and nitro compounds, generally thought to be associated with photochemical production. Delta analysis can also be segregated based on estimated fragment carbon number, allowing an indication of the most likely size and/or lability of the molecules being analyzed. *Bahreini et al.* [2005] showed in chamber experiments that Δ values shift from positive to negative for SOA from biogenic species as molecular size of the fragment increases.

[35] The average relative intensities of Δ values for the aerosol sampled during ICARTT at Thompson Farm are shown in Figure 6a. A similar figure is shown by *Bahreini et al.* [2005] (Figure 15c in that paper) for background pollution aerosol in Ohio during ICARTT. Comparing the two, it is clear that the dominant Δ pattern was consistent between the two sample sites: $\Delta = 2 > \Delta = 0 > \Delta = 3 > \Delta = -1$. At this point, the patterns diverged, with increased relative importance of $\Delta = -2$ and $\Delta = -4$ and decreased

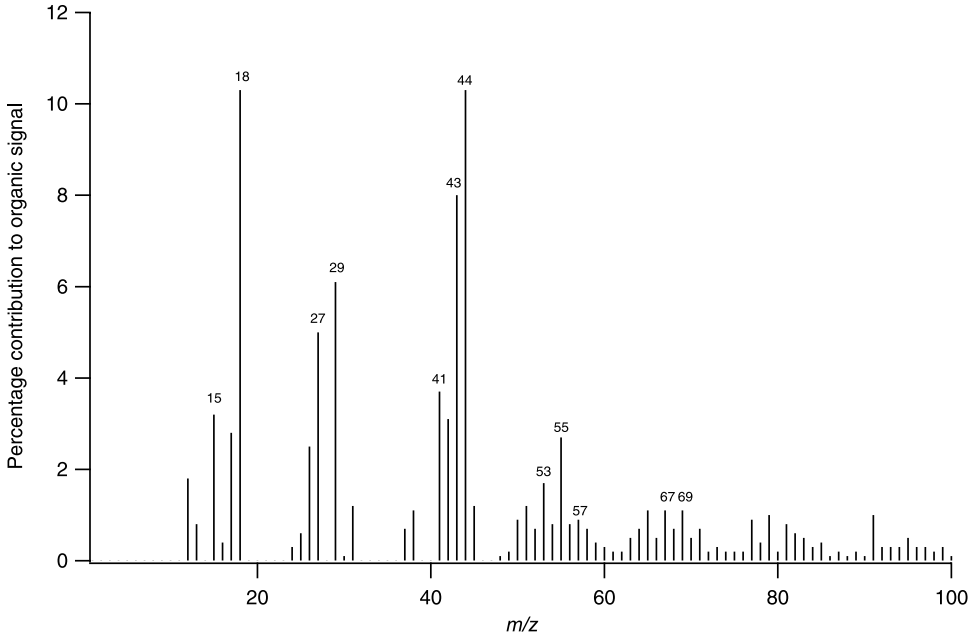

Figure 5. Average contribution of specific *m/z* values to the total organic signal over the course of ICARTT at Thompson Farm.

relative importance of $\Delta = 1$ and $\Delta = 4$ in the pattern from the samples taken at Thompson Farm. This is consistent with an increased importance of negative Δ values for SOA formed from biogenic precursors [*Bahreini et al.*, 2005]. However, this shift may not be attributed solely to biogenic SOA because such a shift is also consistent with biomass burning aerosols [*Bahreini et al.*, 2005, Figure 15a].

[36] The average Δ values segregated by fragment size for the aerosol sampled during ICARTT at Thompson Farm are indicated in Figure 6b. As with the average delta patterns in Figure 6a, comparisons of these values can be made to those for aerosols sampled during a biomass burning event and in urban and rural Ohio during ICARTT [*Bahreini et al.*, 2005, Figure 16]. In general, the patterns are all similar in that the smallest fragments (C_1-C_4) had a positive average Δ value slightly smaller than 1.0 and that larger C_5–C_6 and C_7–C_{15} fragments exhibited negative average Δ values (generally on the order of -1.0). Only in the case of aerosols sampled at Thompson Farm was the average Δ value associated with the C_5-C_6 fragments more negative than the average Δ value associated with the C_7-C_{15} fragments. This is consistent with SOA from the oxidation of the monoterpenes α-pinene and myrcene in chamber studies [*Bahreini et al.*, 2005].

4.3. OA/CO

[37] Evidence to support an anthropogenic source of OA at Thompson Farm is illustrated in Figure 7, which indicates the time series of total OA mass loadings and the anthropogenic indicators CO and BC, the latter two of which are correlated with $R^2 = 0.73$. The correlation coefficients between organic material and CO and BC are $R^2 = 0.59$ and $R^2 = 0.58$, respectively. This indicates a significant relationship, though not one that captures all variability in observed OA mass loadings, as would be expected due to formation of SOA. These values are comparable to the regression coefficient, $R^2 = 0.55$, between CO and WSPOC observed by *Sullivan et al.* [2006] in the lower two kilometers of the troposphere over New England during ICARTT. If it is assumed based on this relationship that the dominant OA source is, in fact, anthropogenic, the correlations with CO and BC yield little information about whether the organic aerosol is primary or secondary.

[38] *Sullivan et al.* [2006] investigated the ratio of the increase in WSPOC concentration relative to a background level to the corresponding increase of CO mixing ratio in very distinct urban plumes in the lower two kilometers of the troposphere. For fresh emissions, the ratio of OC to CO is approximately 1 μg C m^{-3} $ppmv^{-1}$ [*Kirchstetter et al.*, 1999]. *Sullivan et al.* [2006] observed a range of 3 to 32 μg C m^{-3} $ppmv^{-1}$, with the smaller values representing fresher emissions and the larger ones representing air masses with a photochemical age of approximately one day. Similar analyses have been performed for this study. However, it should be noted that the measurements of both *Kirchstetter et al.* [1999] and *Sullivan et al.* [2006] were based on carbon only. In addition, the aerosol measured by *Sullivan et al.* [2006] constituted only the water soluble portion. For comparison to the data collected in this study, the range of 3 to 32 μg C m^{-3} $ppmv^{-1}$ observed by *Sullivan et al.* [2006] was converted to a range of 9 to 99 μg m^{-3} $ppmv^{-1}$ using a conversion factor of 3.1 to account for non-water-soluble and non-carbon organic mass [*Peltier et al.*, 2007].

[39] For such an analysis, it is necessary to determine the background OA concentration and CO mixing ratio so that increases over these levels can be calculated. For this study, the background levels are defined as the fifth percentile of the OA and CO data for the period during which the Q-AMS sampled. For OA, this value was 1.5 μg m^{-3}; the corresponding CO mixing ratio was 115 ppbv. For compar-

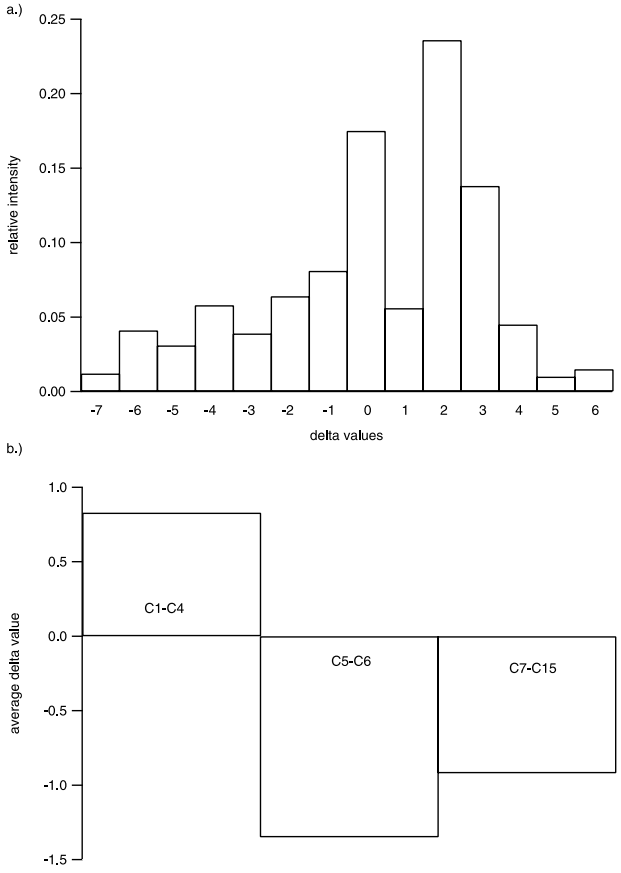

Figure 6. (a) The average relative intensities of Δ values for the OA sampled at Thompson Farm over the course of the ICARTT campaign. (b) The average Δ values segregated by probable molecular size for the OA sampled at Thompson Farm over the course of the ICARTT campaign.

ison, the values used by *Sullivan et al.* [2006] were 0.75 μg C m^{-3} (which is equivalent to 2.3 μg m^{-3} based on the adjustment factor of 3.1) and 121 ppbv, respectively, values slightly larger but not vastly different than those used in the current study. The ratio used in the present study was calculated as:

$$\left(\frac{\Delta OA}{\Delta CO}\right)_t = \left(\frac{OA_t - 1.5}{CO_t - 115}\right)1000 \qquad (2)$$

where OA_t (μg m^{-3}) and CO_t (ppbv) represent the measured concentration or mixing ratio at the time at which the ΔOA/ΔCO ratio (μg m^{-3} ppmv^{-1}) is calculated. Again, it should be stressed that the calculations performed here are not specific to urban plumes, in contrast to *Sullivan et al.* [2006].

[40] In the following statistical discussion, values calculated from equation (2) are included only if the OA concentration and the CO mixing ratio were both at least 1.5 times as large as the calculated respective background values. Over the course of ICARTT, the average value of ΔOA/ΔCO calculated from measurements at Thompson Farm was 72.7 ± 36.5 (SD) μg m^{-3} ppmv^{-1}, and the corresponding range was 6.7 to 227.0 μg m^{-3} ppmv^{-1}. The median ratio was 63.3 μg m^{-3} ppmv^{-1}. The 5th, 25th, 75th, and 95th percentiles of the ratio at Thompson Farm during ICARTT were 27.7, 49.3, 87.9, and 151.5 μg m^{-3} ppmv^{-1}, respectively. The average value is only 27% less than the maximum of the corrected range observed by *Sullivan et al.* [2006] in urban plumes over the course of one day of photochemical aging, which was noted to be very similar to that measured by *deGouw et al.* [2005]. Uncertainties in the respective aerosol measurements make the values reported here and those reported by *Sullivan et al.* [2006] agree more closely.

[41] Based on the source region analysis described using HYSPLIT, it is also possible to investigate the statistics of the ΔOA/ΔCO ratio for periods likely influenced by pollution, representative of background conditions, and characterized by biomass burning. The average ΔOA/ΔCO ratio for periods influenced by pollution was 83.0 ± 41.7 (SD) μg m^{-3} ppmv^{-1}, that for background conditions was 56.8 ± 19.9 (SD) μg m^{-3} ppmv^{-1}, and that for biomass burning conditions was 56.6 ± 9.9 (SD) μg m^{-3} ppmv^{-1}. The values presented here for pollution influenced conditions are close but slightly enhanced compared to the overall data set average of 72.7 ± 36.5 (SD) μg m^{-3} ppmv^{-1}, with comparable standard deviations. The values for background and periods influenced most strongly by biomass burning clearly show comparatively less OA enhancement relative to CO.

[42] The ΔOA/ΔCO ratio is plotted in Figure 8a versus time and shaded by photochemical age, τ, which is calculated as [*Roberts et al.*, 1984]

$$\tau = \frac{1}{3600[OH](k_t - k_b)}\left\{\ln ER - \ln\left(\frac{[\text{toluene}]}{[\text{benzene}]}\right)\right\} \qquad (3)$$

where brackets represent concentrations or mixing ratios of the relevant species with [OH] assumed to be 3 × 10^6 molecules cm^{-3} based on *Warneke et al.* [2004] and toluene and benzene mixing ratios measured by PTR-MS, k_t and k_b are the reaction rate coefficients with OH for toluene and benzene (cm^3 molecules^{-1} sec^{-1}), respectively, and *ER* is the emission ratio of toluene to benzene, here taken to be 3.7 based on *deGouw et al.* [2005]. Temperature-independent (at 298 K) rate constants are taken from *Atkinson and Arey* [2003], as in the work by *deGouw et al.* [2005]. It should be stressed that this calculation of photochemical age does not take into account physical mixing or loss processes, photochemical aging as the result of the presence of biogenic VOCs, and temperature variations affecting the values of the toluene and benzene rate constants with OH. In Figure 8a, data points are included only for those times at which the toluene and benzene mixing ratios were both greater than the respective 5th percentile values for the ICARTT campaign.

[43] Figure 8a clearly shows that large ΔOA/ΔCO ratios are associated with photochemical ages that would be consistent with fresh anthropogenic emissions. This indicates that the high ΔOA/ΔCO values associated with Thompson Farm are likely a result of a regional surface OA signal into which fresh, local emissions are mixed. This regional OA signal could result from anthropogenic POA

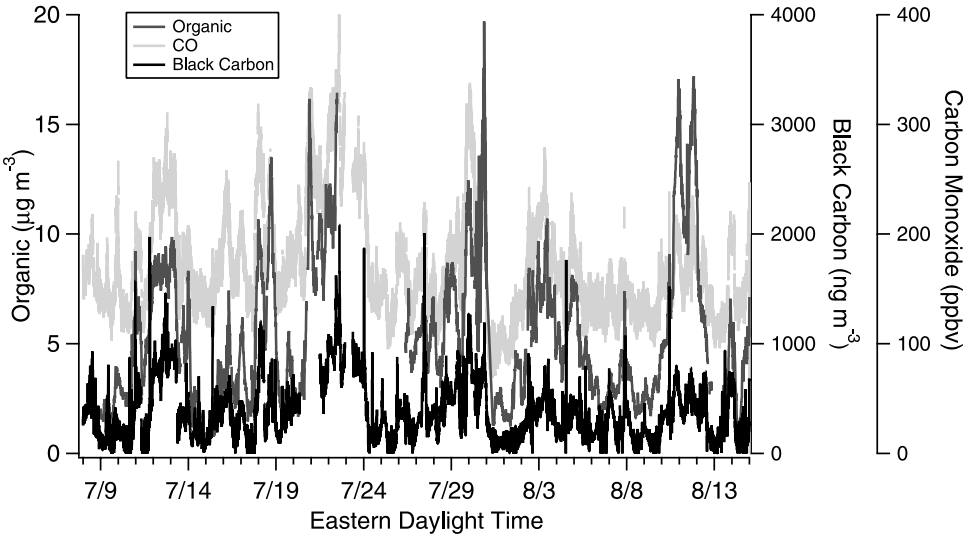

Figure 7. CO mixing ratios (ppbv), BC concentrations (ng m^{-3}), and Q-AMS-measured OA loadings (μg m^{-3}) at Thompson Farm during ICARTT.

emitted far upwind, aged SOA, and local SOA. The contributions of different types of OA will be discussed below.

[44] The hypothesized impact of multiple types of sources is supported by Figure 8b which indicates the ΔOA/ΔCO values over time but shaded instead by the ratio of the sum of the mixing ratios of methacrolein and methyl-vinyl-ketone (MACR and MVK, respectively) to the mixing ratio of isoprene (all measured with PTR-MS) as an indicator of aging with respect to biogenic hydrocarbons. MACR and MVK are known isoprene oxidation products. Such ratios greater than approximately 0.54 indicate significant photochemical processing [*deGouw et al.*, 2005]. In Figure 8b, data points are included only for those times at which the isoprene and MVK and MACR mixing ratios were both greater than the respective 5th percentile values for the ICARTT campaign. As with the relationship to anthropogenic aromatics shown in Figure 8a, Figure 8b indicates no relationship between ΔOA/ΔCO and age with respect to isoprene. Unfortunately, no measurements of monoterpene oxidation products were made at Thompson Farm during ICARTT so a similar analysis with monoterpenes is not possible.

[45] It should also be noted that a scatterplot of ΔOA/ΔCO versus either measure of photochemical age (not shown) indicates no plateau of these values with increasing photochemical age, as was observed by *Sullivan et al.* [2006] in urban plumes. This could indicate a lack of proximate sources, favorable addition of OA to the air masses measured at Thompson Farm due to chemistry not occurring in the urban plumes analyzed in the previous studies [*deGouw et al.*, 2005; *Sullivan et al.*, 2006], or both.

[46] Figure 8 also indicates the behavior of the ΔOA/ΔCO ratio as a function of source region (influenced, background, or biomass burning). It is clear in both parts of Figure 8 that no strong relationship between this ratio and source region is observed. This is in direct contrast to the data of *Sullivan et al.* [2006], likely due to site-specific surface characteristics associated with Thompson Farm. These differences likely are enhanced by the fact that *Sullivan et al.* [2006] focused their analyses on distinct urban plumes while this study focused on a fixed surface site influenced by many air mass types.

4.4. Multivariate Statistical Analyses

[47] A multiple component analysis (MCA) technique, which is an extended version of the custom principal component analysis developed by *Zhang et al.* [2005c], has been developed to separate Q-AMS-measured organic material into several components, typically representing OOA of different types and hydrocarbon-like OA (HOA) [*Zhang et al.*, 2007b]. The MCA is initialized with the average OA mass spectrum of the entire study and applies a hierarchical alternative multiple linear regression algorithm to deconvolve the components based on analyses of the residual matrix [*Zhang et al.*, 2006]. The result is the best fit statistical contribution of several OA components, each represented by a separate, time-invariant spectrum, to the overall OA concentration measured by the Q-AMS.

[48] When MCA was applied to the ICARTT data set from Thompson Farm, three OOA components that showed varying level of oxidation (based on the appearance of the spectra) were identified, along with an HOA component that appeared to contain significant contribution from biomass burning OA (BBOA, see below). While this solution was mathematically optimal, two of the OOA components had very similar time series and mass spectra that were separately unrealistic, which is characteristic of component splitting due to variability in the mass spectra (I. M. Ulbrich et al., Interpretation of organic components from positive matrix factorization of aerosol mass spectrometric data, submitted to *Atmospheric Chemistry and Physics Discussions*, 2008). The component obtained by summing these two components likely represents a temporally joint component that varies in terms of age. Therefore these two OOA components were combined linearly into one (OOA-II), and the average mass spectrum, its 1σ variations, and a time series are reported in Figure 9.

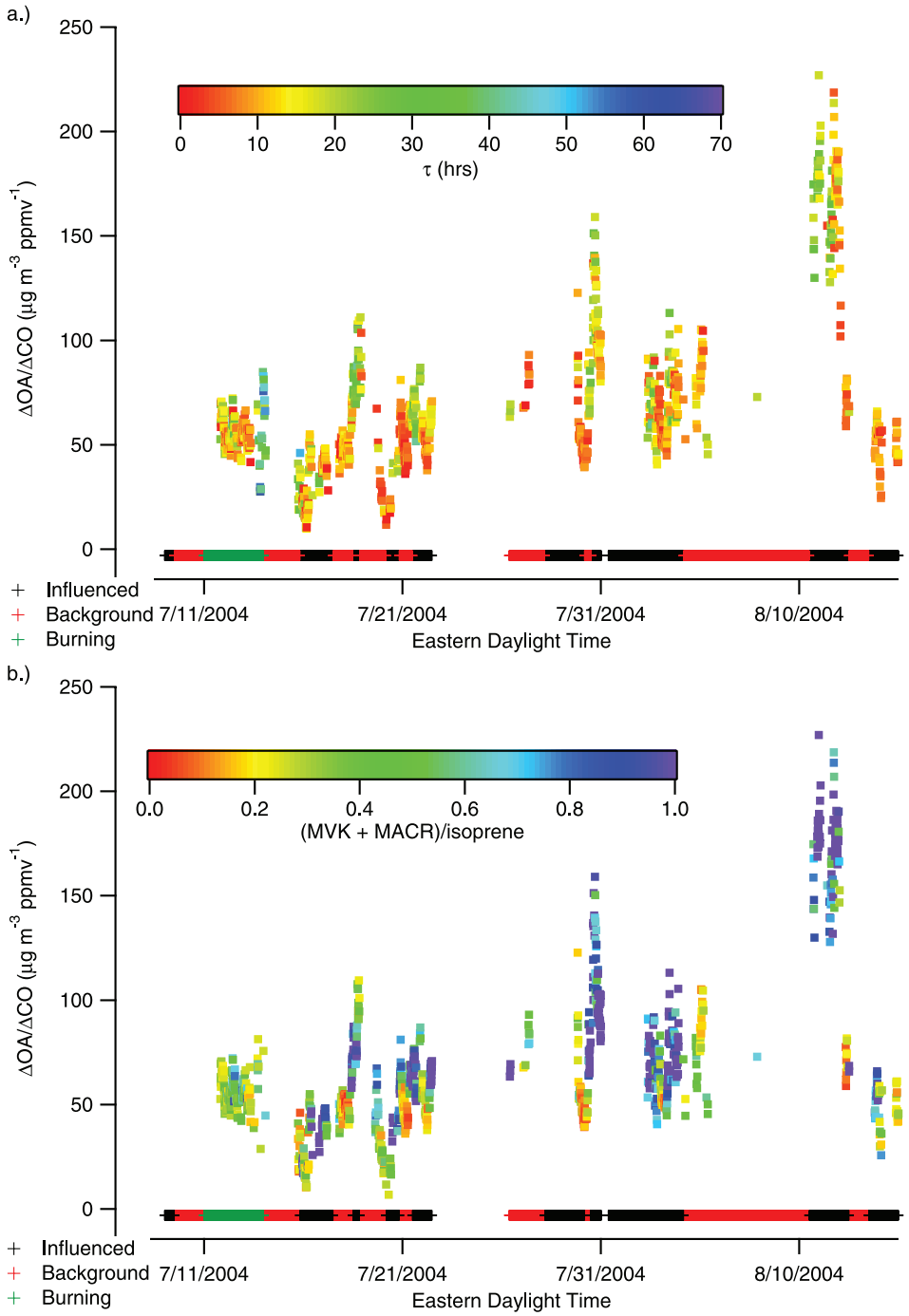

Figure 8. (a) $\Delta OA/\Delta CO$ ($\mu g\ m^{-3}\ ppmv^{-1}$) at Thompson Farm over the course of ICARTT as calculated by equation (2). Points are shaded by estimated photochemical age, τ (h), as calculated by equation (3). (b) The same plot shaded by (MVK+MACR)/isoprene. Source regions are defined in the text as influenced (black), background (red), or burning (green) and are indicated by the stripe along the bottom of the diagram.

[49] Also shown in Figure 9 are the mass spectra of the other two components (HOA/BBOA and OOA-I) and their time series over the ICARTT campaign. The OOA components are denoted as OOA-I and OOA-II in reverse order of level of oxidation (based on the appearance of the spectra) for historical reasons as the more oxidized OOA components were identified first [*Zhang et al.*, 2005b, 2005c] while less oxidized OOA components have been identified more recently [*Zhang et al.*, 2007b; *Lanz et al.*, 2007; *Nemitz et al.*, 2008]. The mass spectrum of OOA-I has a higher ratio of *m/z* 44 to *m/z* 43 than OOA-II. Note that the OOA components are sorted by apparent oxidation in each study. That is, OOA-II here may not correspond to the same sources or have the same volatility or other properties as the OOA-II observed in other studies, such as those of *Lanz et al.* [2007], *Nemitz et al.* [2008], and Ulbrich et al. (submitted manuscript, 2008). As indicated in Figure 9, during a major pollution event in the mid-August, OOA-I clearly dominates. Averaged over the campaign, the three components had average mass contributions to OA of 1.1 μg m^{-3}, 1.3 μg m^{-3}, and 2.9 μg m^{-3} for HOA/BBOA, OOA-I, and OOA-II, respectively. These values represent average mass-based compositions of OA of 21%, 24%, and 55%, respectively.

[50] The OA spectra from the Q-AMS from this study have also been analyzed using positive matrix factorization (PMF) in a manner similar to that used by *Lanz et al.* [2007], who also give an overview of the PMF methodology and its inherent strengths and issues. Similar to MCA, PMF allows for a statistical investigation of the various sources that affect OA levels in a Q-AMS data set. Because the results of the MCA and the PMF analyses are broadly consistent with one another, only the MCA results are discussed here. It should be noted that the factors and components found in this data set are significantly correlated in time (and in mass spectra for the two OOAs) and that these are the hardest type of data for these types of factorization techniques to separate (Ulbrich et al., submitted manuscript, 2008). As a result, the different OOA components may not just represent different precursors (biogenic versus anthropogenic) or source regions (continental versus more local) but also variable degrees of aging.

[51] While specific statistical analyses using the HOA/BBOA, OOA-I and OOA-II components are discussed below, their general characteristics are addressed here. The HOA/BBOA component correlates well with BC and CO (R^2 = 0.76 and 0.79, respectively) and has a spectrum similar, but not equivalent, to that of HOA observed in urban environments (enhanced signals at *m/z* 41, 43, 55, 57 and 91), likely due to post-emission oxidation [*Zhang et al.*, 2005a, 2005b]. This component also has markings of the influence of BBOA (enhanced signals at *m/z* 60 and 73 from levoglucosan and related compounds [*Schneider et al.*, 2006]). Component OOA-I correlates well with sulfate aerosol (R^2 = 0.74) and has a spectrum very similar to OOA observed during PAQS (R^2 = 0.97) [*Zhang et al.*, 2005a, 2005b], though slightly more oxidized (enhanced signals at *m/z* 18, 29, and 44), likely due to stronger photochemistry during the summer months. Finally, component OOA-II correlates with the HOA/BBOA component quite well (R^2 = 0.72), but the spectrum is marked by some similarity to biogenic SOA (enhancement of signal at *m/z* 43 relative to *m/z* 44) [*Bahreini et al.*, 2005], raising the possibility of enhanced biogenic SOA formation under polluted conditions as suggested by the field measurements of *deGouw et al.* [2005] and the modeling study of *Tsigaridis and Kanakidou* [2007].

[52] Table 1 displays the Pearson *R* coefficient for regression of the three components identified by the method of *Zhang et al.* [2007b], ammonium, nitrate, and sulfate with O_3, NO, NO_2, CO, BC, VOCs, oxygenated VOCs, and halocarbons. In Table 1, those coefficients with a value greater than or equal to 0.6 are shown in bold. Those gases measured by PTR-MS, as opposed to GC-FID, are shown in italic font.

[53] The bold font used in Table 1 clearly indicates groupings of species that are correlated more strongly to the Q-AMS-measured or derived aerosol species. For example, the HOA/BBOA component shows very strong correlation to CO, BC, the series of *n*- and branched alkanes up to those with eight carbon atoms, ethyne, the series of aromatic compounds, and the series of alkyl nitrates. These relationships clearly indicate the probability that this component may be a surrogate for POA, including that associated with BBOA, despite a weak relationship with acetonitrile.

[54] The OOA-II component showed similar relationships as did the HOA/BBOA component but to a lesser degree in terms of strength of the correlations. Given the spectral characteristics of the two extracted components that were linearly combined to determine OOA-II, it is likely, though not certain, that this component appears to be a mixture of continental background SOA and regional/local production of SOA. It should also be noted that the relationships between the organic components and the alkyl nitrates are significantly weaker than that observed by *deGouw et al.* [2005] (R^2 = 0.69) on the RV *Ronald H. Brown* between iso-propyl nitrate and total OA during NEAQS; this relationship was used as an indicator of anthropogenic SOA in that study. In this study, the relationship between OA and individual alkyl nitrates did not have R^2 values that exceeded 0.44.

[55] In contrast, component OOA-I, sulfate, and ammonium did not show a single strong relationship to the gas-phase species discussed here, indicating the likely regional nature of this material. The regional nature of this aerosol is underscored by the regression coefficient between sulfate and total OA, R^2 = 0.4, which is equal to that observed during PAQS [*Zhang et al.*, 2005a]. In addition, a regression between OOA and sulfate during PAQS yielded a value for R^2 = 0.74, which is equivalent to that between OOA-I and sulfate during ICARTT. Slopes for these regressions (forced through zero) are also very close, 0.35 between OOA-I and sulfate during ICARTT and 0.38 between total OOA and sulfate during PAQS.

[56] Table 2, in which the relationships between the three organic components and nitrate, ammonium, and sulfate, as well as their relationships with each other, are described quantitatively, underscores the stark difference between component OOA-I and the other organic components. As in Table 1, the strongest relationships, those with *R* values greater than or equal to 0.6, are shown in bold. As would be expected based on the discussion above, component OOA-I has strong relationships with sulfate and ammonium aero-

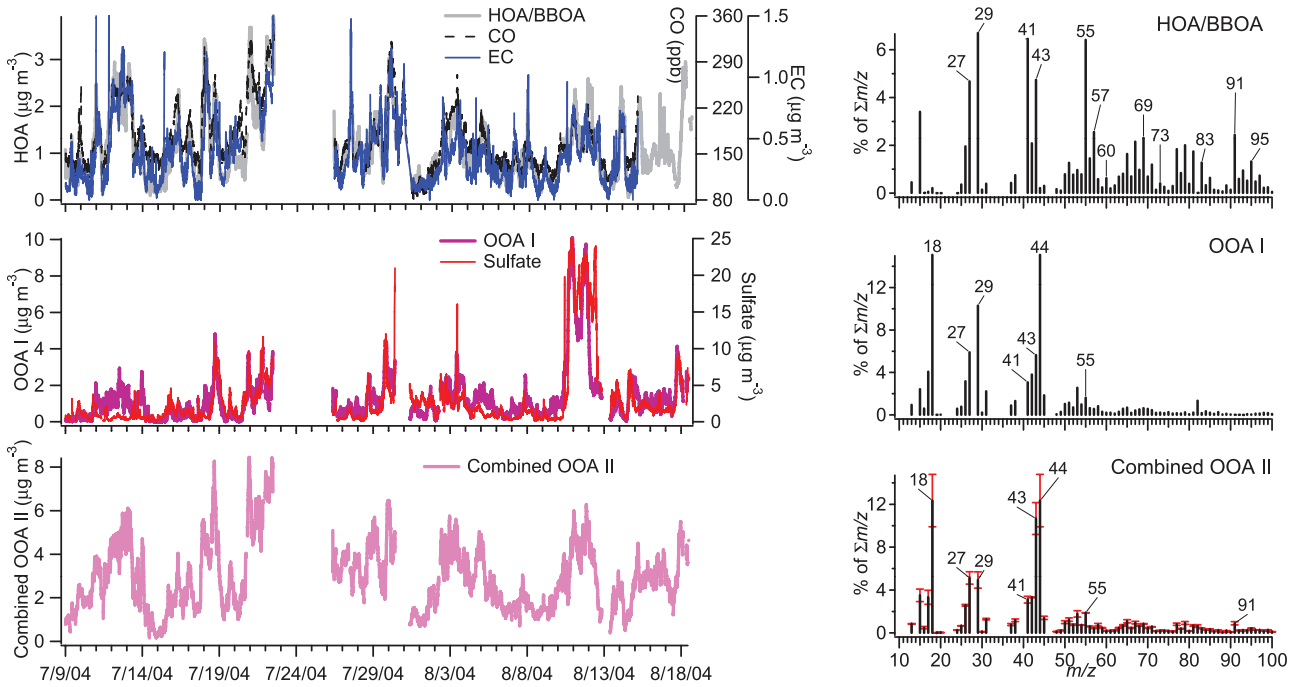

Figure 9. Time series for the components contributing to OA mass loadings at Thompson Farm over the course of the ICARTT campaign as identified by the MCA technique of *Zhang et al.* [2007b]. For comparison, time traces of CO and EC are shown with that of HOA/BBOA and that of sulfate aerosol is shown with OOA-I. The extracted mass spectrum for each of the components is shown to the right of its time series. Combined OOA-II represents the sum of two components extracted by MCA that appear to be the split of an OOA component with varying degree of oxidation over the course of this study. The mass spectrum of Combined OOA-II is determined by linear combination of two split components, and the error bars (in red) indicate the variability (1σ) of this spectrum during the entire study.

sol; in contrast the HOA/BBOA component and component OOA-II show the strongest relationships to nitrate aerosol. The inter-relationships among the components show the OOA-I component to be least correlated to the other two OA components, which is evident in Figure 9 as well.

4.5. Comparison to NEAQS and Other Measurements During ICARTT

[57] The less apparent influence of anthropogenic SOA formation on OA at Thompson Farm during ICARTT is somewhat in contrast to the work of *deGouw et al.* [2005], *Marcolli et al.* [2006], and *Quinn et al.* [2006] in which statistical/modeling techniques were used to estimate that anthropogenic SOA dominated OA concentrations in the surface marine boundary layer off the coast of New England during NEAQS and ICARTT. The results presented here are also in contrast to the observations of *Sullivan et al.* [2006] discussed previously in which large enhancements of WSPOC compared to CO were observed only in urban plumes.

[58] The data shown here are, however, in line with sampling performed at two other land-based coastal sites during ICARTT. Measurements of particle size distributions and VOCs on Appledore Island in the Gulf of Maine indicate the contribution of photochemical oxidation of α- and β-pinene to nanoparticle growth [*Russell et al.*, 2007]. Air quality measurements made using a Q-AMS, a PTR-MS, and a gas chromatographic system at Chebogue Point, Nova Scotia, point to the mixed influence of biogenic and anthropogenic sources to OA concentrations. Like at Thompson Farm, the OA at Chebogue Point is highly oxidized, and periods of biogenic influence at Chebogue Point are characterized by low sulfate aerosol to OA ratios. Chebogue Point aerosols are also characterized by a non-ammonium nitrate signal at *m/z* 30 [*Holzinger et al.*, 2007; *Williams et al.*, 2007; J. D. Allan et al., manuscript in preparation, 2008]. It should be stressed, however, that Chebogue Point is located significantly further from anthropogenic emission sources in the Ohio River valley and along the eastern coast of the United States than is Thompson Farm.

[59] This comparison indicates that the contributions to OA loadings can vary significantly within a given region depending on specific sampling location. In the marine boundary layer of the Gulf of Maine, OA appears to be predominately SOA of anthropogenic origin [*deGouw et al.*, 2005; *Marcolli et al.*, 2006; *Quinn et al.*, 2006]. In the lower free troposphere, measurements show highest levels of WSPOC enhancements in urban areas [*Sullivan et al.*, 2006]. As would be expected, the fixed surface location described here likely is influenced significantly by biogenic and anthropogenic, as well as primary and secondary, processes. It is possible that conditions specific to the environment surrounding Thompson Farm lead to these

Table 1. Pearson *R* Coefficients for Regressions Between Q-AMS Measured/Derived Ammonium, Nitrate, Sulfate, and Organic Components and Other Species Measured at Thompson Farm During ICARTT

	HOA/BBOA	OOA-I	Combined OOA-II	Ammonium	Nitrate	Sulfate
Ozone	−0.15	0.46	0.04	0.34	−0.07	0.40
NO	0.14	−0.08	0.09	0.03	0.10	0.00
NO_2	0.59	0.05	0.44	0.21	0.46	0.15
CO	**0.89**	0.31	**0.79**	0.26	**0.70**	0.20
BC	**0.87**	0.37	**0.73**	0.31	**0.68**	0.26
Methane	0.28	0.05	0.25	0.05	0.22	0.03
Ethane	**0.72**	0.43	**0.66**	0.38	**0.64**	0.35
Propane	**0.71**	0.06	0.58	0.08	**0.61**	0.01
i-Butane	**0.79**	0.11	**0.62**	0.15	**0.66**	0.08
n-Butane	**0.80**	0.14	**0.63**	0.17	**0.66**	0.10
Cyclopentane	**0.77**	0.00	0.58	0.03	0.57	−0.04
i-Pentane	**0.79**	0.09	**0.61**	0.13	**0.62**	0.05
n-Pentane	**0.77**	0.10	0.59	0.13	**0.62**	0.05
Methylcyclopentane	**0.76**	0.03	0.56	0.04	0.57	−0.04
Cyclohexane	**0.71**	0.02	0.50	0.00	0.53	−0.07
n-Hexane	**0.79**	0.11	**0.61**	0.13	**0.65**	0.05
Methylcyclohexane	**0.74**	0.06	0.57	0.09	0.59	0.02
n-Heptane	**0.78**	0.11	**0.63**	0.12	**0.66**	0.05
2,2,4-Trimethylpentane	**0.76**	0.18	**0.65**	0.10	0.53	0.05
2,3,4-Trimethylpentane	**0.72**	−0.02	0.51	−0.03	0.47	−0.08
2-Methylheptane	**0.68**	0.05	0.48	0.05	0.53	−0.01
n-Octane	**0.71**	0.07	0.51	0.04	0.50	0.00
n-Decane	0.56	0.07	0.39	0.04	0.42	−0.02
Ethene	**0.62**	−0.03	0.39	−0.07	0.41	−0.12
Propene	0.58	0.06	0.37	−0.06	0.39	−0.10
t-2-Butene	0.17	0.36	0.02	−0.08	−0.08	−0.11
1-Butene	0.51	0.00	0.31	−0.08	0.30	−0.11
i-Butene	0.59	−0.04	0.37	−0.07	0.35	−0.11
c-2-Butene	0.16	0.11	0.10	−0.11	−0.08	−0.12
t-2-Pentene	0.34	0.13	0.22	0.00	0.16	−0.03
c-2-Pentene	0.30	0.05	0.17	−0.08	0.10	−0.12
2-Methyl-2-butene	0.28	0.17	0.33	0.15	0.19	0.11
1-Pentene	0.58	0.10	0.40	0.02	0.38	−0.02
Ethyne	**0.88**	0.20	**0.71**	0.17	**0.68**	0.10
Benzene	**0.86**	0.20	**0.66**	0.12	**0.63**	0.05
Toluene	**0.75**	0.10	0.59	0.14	**0.64**	0.06
Ethylbenzene	**0.75**	0.11	0.59	0.15	**0.64**	0.07
m & *p*-Xylene	**0.72**	0.05	0.55	0.10	**0.60**	0.02
Styrene	**0.60**	0.02	0.45	0.05	0.46	−0.01
o-Xylene & nonane	**0.68**	0.01	0.51	0.03	0.53	−0.04
m-Ethyltoluene	**0.64**	0.04	0.47	0.02	0.54	−0.05
p-Ethyltoluene	**0.65**	0.08	0.49	0.04	0.53	−0.02
o-Ethyltoluene	0.56	−0.03	0.38	−0.03	0.43	−0.08
1,3,5-Trimethylbenzene	0.56	0.06	0.37	0.01	0.45	−0.04
1,2,4-Trimethylbenzene	**0.62**	0.03	0.44	0.01	0.52	−0.06
1,2,3-Trimethylbenzene	0.58	0.15	0.47	0.06	0.43	0.01
Isoprene	0.32	0.10	0.26	0.03	0.13	0.02
α-Pinene	0.47	−0.01	0.35	−0.06	0.29	−0.09
β-Pinene	0.46	−0.01	0.33	−0.06	0.30	−0.10
Camphene	0.55	−0.01	0.42	−0.02	0.39	−0.07
Limonene	0.52	0.02	0.45	−0.01	0.30	−0.04
Methyl bromide	0.00	0.12	−0.03	0.17	0.07	0.17
Methyl iodide	0.36	0.10	0.24	0.28	0.40	0.26
Dibromomethane	0.29	−0.13	0.17	0.00	0.26	−0.03
Tribromomethane	0.45	−0.08	0.35	0.03	0.41	−0.02
Tetrachloroethylene	**0.68**	0.20	**0.62**	0.29	**0.66**	0.22
Trichloroethylene	0.51	0.04	0.41	0.13	0.59	0.06
Chloroiodomethane	0.00	0.26	−0.01	0.44	0.12	0.43
Methyl nitrate	0.39	0.33	0.43	0.43	0.45	0.41
Ethyl nitrate	0.54	0.36	0.57	0.43	0.57	0.39
1-Propyl nitrate	**0.60**	0.37	**0.64**	0.45	**0.64**	0.40
2-Propyl nitrate	**0.60**	0.38	**0.64**	0.47	**0.65**	0.42
2-Butyl nitrate	0.56	0.41	**0.62**	0.48	**0.64**	0.43
3-Pentyl nitrate	**0.63**	0.34	**0.66**	0.39	**0.64**	0.34
2-Pentyl nitrate	**0.62**	0.37	**0.66**	0.42	**0.64**	0.36
Acetonitrile	*0.16*	*0.19*	*0.27*	*0.03*	*0.00*	*0.03*
Dimethyl sulfide	*0.01*	*−0.12*	*−0.13*	*−0.04*	*−0.07*	*−0.04*
Methanol	*0.14*	*0.37*	*0.28*	*0.19*	*0.08*	*0.20*

Table 1. (continued)

	HOA/BBOA	OOA-I	Combined OOA-II	Ammonium	Nitrate	Sulfate
Acetaldehyde	*0.33*	*0.37*	*0.40*	*0.18*	*0.19*	*0.18*
Acetone	*0.49*	*0.48*	***0.63***	*0.29*	*0.36*	*0.28*
Methyl ethyl ketone	*0.40*	*0.35*	*0.49*	*0.19*	*0.26*	*0.19*
Acetic acid	*0.06*	*0.39*	*0.23*	*0.21*	*0.07*	*0.25*

differences and that this influence is diluted upon transport away from the site.

5. Conclusions

[60] An Aerodyne Q-AMS operated at the UNH Atmospheric Observatory at Thompson Farm during ICARTT indicates that the submicron, non-refractory aerosol mass in summer at this location is dominated by sulfate and organic material. Ammonium aerosol concentrations track closely those of sulfate aerosol, while nitrate concentrations typically track closely those of OA. Highest aerosol concentrations are transported from the southwest.

[61] Independent methods have been used to investigate the contribution of various types of aerosol to the OA burden at Thompson Farm. An OA/BC analysis indicates that the bulk of the measured OA is secondary in nature at Thompson Farm during summer, with spectral analyses confirming its aged and oxidized nature. The relationship between OA and CO provides evidence that surface forested sites may show enhancements of OA relative to CO compared to studies in urban plumes. Component and factor analyses distinguished between three types of OA: HOA/BBOA and two types of OOA of different levels of oxidation, likely representing different sets of both local and distant sources/processes. These two different types of OOA likely are influenced by both anthropogenic and biogenic sources based on both comparison to gas-phase data and spectral characteristics. However, based on the available information, an unequivocal way to separate anthropogenic and biogenic OOA from only Q-AMS measurements at locations such as Thompson Farm with large regional contributions to OA is currently lacking, especially given the possibility of anthropogenic activity enhancing biogenic SOA formation.

[62] **Acknowledgments.** Financial support for this work was provided in part by the Office of Oceanic and Atmospheric Research of NOAA under AIRMAP grants NA03OAR4600122 and NA04OAR4600154 and in part by the National Science Foundation under grant ATM-0327643. JLJ, IU, and QZ acknowledge support from the USEPA under grant RD-83216101-0. Any opinions, findings, and conclusions or recommendations expressed in this material are those of the authors and do not necessarily reflect the views of the funding agencies. The authors would also like to thank James Allan and the entire Q-AMS community for provision of and continued improvements to Q-AMS data analysis software, with specific thanks to Manjula Canagaratna and Tim Onasch for development and improvement of the ion series/delta analysis package. Our gratitude also goes to John Jayne and Doug Worsnop for their assistance in installation of and training on the Q-AMS. We also thank Roya Bahreini for helpful discussion regarding delta analysis, Jack Dibb for useful discussions, Chuck Brock, Hugh Coe, Allen Goldstein, and Kostas Tsigaridis for provision of unpublished manuscripts, and the AIRMAP project team for continued operation and maintenance of the UNH Atmospheric Observatories. Members of the Sive group provided assistance with generation of the VOC data used in this manuscript. The authors gratefully acknowledge the NOAA Air Resources Laboratory (ARL) for the provision of the HYSPLIT transport and dispersion model (http://www.arl.noaa.gov/ready.html) used in this publication. We would like to thank anonymous reviewers whose comments greatly improved the scientific analyses included in this paper.

Table 2. Pearson *R* Coefficients for Regressions Between Q-AMS Derived Organic Components and Q-AMS Measured/Derived Sulfate, Nitrate, Ammonium, and Organic Components

	HOA/BBOA	OOA-I	Combined OOA-II
Sulfate	0.31	**0.86**	0.38
Nitrate	**0.80**	0.58	**0.77**
Ammonium	0.34	**0.83**	0.45
HOA/BBOA	–		
OOA-I	0.45	–	
Combined OOA-II	**0.85**	0.50	–

References

Alfarra, M. R., et al. (2004), Characterization of urban and regional organic aerosols in the Lower Fraser Valley using two aerodyne aerosol mass spectrometers, *Atmos. Environ.*, *38*, 5745–5758.

Alfarra, M. R., D. Paulsen, M. Gysel, A. A. Garforth, J. Dommen, A. S. H. Prevot, D. R. Worsnop, U. Baltensperger, and H. Coe (2006), A mass spectrometric study of secondary organic aerosols formed from the photooxidation of anthropogenic and biogenic precursors in a reaction chamber, *Atmos. Chem., Phys., 6*, 5279–5293.

Allan, J. D., J. L. Jimenez, P. I. Williams, M. R. Alfarra, K. N. Bower, J. T. Jayne, H. Coe, and D. R. Worsnop (2003), Quantitative sampling using an Aerodyne aerosol mass spectrometer: Part 1: Techniques of data interpretation and error analysis, *J. Geophys. Res.*, *108*(D3), 4090, doi:10.1029/2002JD002358.

Allan, J. D., et al. (2004), Technical note: Extraction of chemically resolved mass spectra from Aerodyne aerosol mass spectrometer data, *J. Aerosol Sci.*, *35*, 909–922.

Atkinson, R., and J. Arey (2003), Atmospheric degradation of volatile organic compounds, *Chem. Rev.*, *103*, 4605–4638.

Bae, M.-S., J. J. Schwab, Q. Zhang, O. Hogrefe, K. L. Demerjian, S. Weimer, K. Rhoads, D. Orsini, P. Venkatachari, and P. K. Hopke (2007), Interference of organic signals in highly-time resolved nitrate measurements by low mass resolution aerosol mass spectrometry, *J. Geophys. Res.*, *112*, D22305, doi:10.1029/2007JD008614.

Bahreini, R., M. D. Keywood, N. L. Ng, V. Varutbangkul, S. Gao, R. C. Flagan, J. H. Seinfeld, D. R. Worsnop, and J. L. Jimenez (2005), Measurements of secondary organic aerosol from oxidation of cycloalkenes, terpenes, and m-xylene using an Aerodyne aerosol mass spectrometer, *Environ. Sci. Technol.*, *39*, 5674–5688.

Brock, C. A., et al. (2004), Particle characteristics following cloud-modified transport from Asia to North America, *J. Geophys. Res.*, *109*, D23S26, doi:10.1029/2003JD004198.

Brock, C. A., et al. (2008), Sources of particulate matter in the northeastern United States in summer: 2. Evolution of chemical and microphysical properties, *J. Geophys. Res.*, doi:10.1029/2007JD009241, in press.

Brown, S. S., et al. (2006), Nocturnal odd-oxygen budget and its implications for ozone loss in the lower troposphere, *Geophys. Res. Lett.*, *33*, L08801, doi:10.1029/2006GL025900.

Chen, J., H. Mao, R. W. Talbot, and R. J. Griffin (2006), Application of the CACM and MPMPO modules using the CMAQ model for the Eastern United States, *J. Geophys. Res.*, *111*, D23S25, doi:10.1029/2006JD007603.

DeCarlo, P., J. G. Slowik, D. R. Worsnop, P. Davidovits, and J. L. Jimenez (2004), Particle morphology and density characterization by combined mobility and aerodynamic diameter measurements. Part 1: Theory, *Aerosol Sci. Technol.*, *38*, 1185–1205.

DeCarlo, P. F., et al. (2006), A field-deployable high-resolution time-of-flight aerosol mass spectrometer, *Anal. Chem.*, *78*, 8281–8289.

deGouw, J. A., et al. (2005), The budget of organic carbon in a polluted atmosphere: Results from the New England Air Quality Study in 2002, *J. Geophys. Res.*, *110*, D16305, doi:10.1029/2004JD005623.

Draxler, R. R., and G. D. Rolph (2003), HYSPLIT (HYbrid Single-Particle Lagrangian Integrated Trajectory) Model access via NOAA ARL READY Website (http://www.arl.noaa.gov/ready/hysplit4.html). NOAA Air Resources Laboratory, Silver Spring, MD.

Drewnick, F., J. J. Schwab, O. Hogrefe, S. Peters, L. Husain, D. Diamond, R. Weber, and K. L. Demerjian (2003), Intercomparison and evaluation of four semi-continuous $PM_{2.5}$ sulfate instruments, *Atmos. Environ.*, *37*, 3335–3350.

Drewnick, F., J. J. Schwab, J. T. Jayne, M. Canagaratna, D. R. Worsnop, and K. L. Demerjian (2004), Measurements of ambient aerosol composition during PTMACS-NY 2001 using an aerosol mass spectrometer. Part I: Mass concentrations, *Aerosol Sci. Technol.*, *38*, 92–103.

Duck, T. J., et al. (2007), Transport of forest fire emissions from Alaska and the Yukon Territory to Nova Scotia during Summer 2004, *J. Geophys. Res.*, *112*, D10S44, doi:10.1029/2006JD007716.

Fehsenfeld, F. C., et al. (2006), International Consortium for Atmospheric Research on Transport and Transformation (ICARTT): North America to Europe: Overview of the 2004 summer field study, *J. Geophys. Res.*, *111*, D23S01, doi:10.1029/2006JD007829.

Fischer, E. V., R. W. Talbot, J. E. Dibb, J. L. Moody, and G. L. Murray (2004), Summertime ozone at Mount Washington: Meteorological controls at the highest peak in the northeast, *J. Geophys. Res.*, *109*, D24303, doi:10.1029/2004JD004841.

Fischer, E. V., L. D. Ziemba, R. W. Talbot, J. E. Dibb, R. J. Griffin, L. Husain, and A. N. Grant (2007), The aerosol major ion record at Mount Washington, *J. Geophys. Res.*, *112*, D02303, doi:10.1029/2006JD007253.

Fugas, M., and M. Gentilizza (1978), Relationship between sulfate and sulfur dioxide in air, *Atmos. Environ.*, *12*, 335–337.

Gard, E. E., et al. (1998), Direct observation of heterogeneous chemistry in the atmosphere, *Science*, *279*, 1184–1187.

Griffin, R. J., C. A. Johnson, R. W. Talbot, H. Mao, R. S. Russo, Y. Zhou, and B. C. Sive (2004), Quantification of ozone formation metrics at Thompson Farm during the New England Air Quality Study (NEAQS) 2002, *J. Geophys. Res.*, *109*, D24302, doi:10.1029/2004JD005344.

Griffin, R. J., P. J. Beckman, R. W. Talbot, B. C. Sive, and R. K. Varner (2007), Deviations from ozone photostationary state during ICARTT 2004: Use of measurements and photochemical modeling to assess causes, *J. Geophys. Res.*, *112*, D10S07, doi:10.1029/2006JD007604.

Harley, R. A., L. C. Marr, J. K. Lehner, and S. N. Giddings (2005), Changes in motor vehicle emissions on diurnal to decadal time scales and effects on atmospheric composition, *Environ. Sci. Technol.*, *39*, 5356–5362.

Hogrefe, O., et al. (2004), Semi-continuous $PM_{2.5}$ sulfate and nitrate measurements at an urban and a rural location in New York: PMTACS-NY summer 2001 and 2002 campaigns, *J. Air Waste Manage. Assoc.*, *54*, 1040–1060.

Holzinger, R., C. Warneke, A. Hansel, A. Jordan, W. Lindinger, D. H. Scharffe, G. Schade, and P. J. Crutzen (1999), Biomass burning as a source of formaldehyde, acetaldehyde, methanol, acetone, acetonitrile, and hydrogen cyanide, *Geophys. Res. Lett.*, *26*(8), 1161–1164.

Holzinger, R., et al. (2007), Emission, oxidation, and secondary organic aerosol formation of volatile organic compounds as observed at Chebogue Point, Nova Scotia, *J. Geophys. Res.*, *112*, D10S24, doi:10.1029/2006JD007599.

Huffman, J. A., J. T. Jayne, F. Drewnick, A. C. Aiken, T. Onasch, D. R. Worsnop, and J. L. Jimenez (2005), Design, modeling, optimization, and experimental tests of a particle beam width probe for the Aerodyne aerosol mass spectrometer, *Aerosol Sci. Technol.*, *39*, 1143–1163.

Intergovernmental Panel on Climate Change (2001), *Climate Change 2001: The Scientific Basis*, edited by J. T. Houghton et al., Cambridge University Press, New York.

Jacob, D. J. (2000), Heterogeneous chemistry and tropospheric ozone, *Atmos. Environ.*, *34*, 2131–2159.

Jaenicke, R. (2005), Abundance of cellular material and proteins in the atmosphere, *Science*, *308*, 73.

Jayne, J. T., D. C. Leard, X. Zhang, P. Davidovits, K. A. Smith, C. E. Kolb, and D. R. Worsnop (2000), Development of an aerosol mass spectrometer for size and composition analysis of submicron particles, *Aerosol Sci. Technol.*, *33*, 49–70.

Jimenez, J. L., et al. (2003), Ambient aerosol sampling with an aerodyne aerosol mass spectrometer, *J. Geophys. Res.*, *108*(D7), 8425, doi:10.1029/2001JD001213.

Kirchstetter, T. W., R. A. Harley, N. M. Kreisberg, M. R. Stolzenburg, and S. V. Hering (1999), On-road measurement of fine particle and nitrogen oxide emissions from light- and heavy-duty motor vehicles, *Atmos. Environ.*, *33*, 2955–2968.

Kleinman, L. I., P. H. Daum, Y. N. Lee, L. J. Nunnermacker, S. R. Springston, J. Weinstein-Lloyd, and J. Rudolph (2005), A comparative study of ozone production in five U.S. metropolitan areas, *J. Geophys. Res.*, *110*, D02301, doi:10.1029/2004JD005096.

Lanz, V. A., M. R. Alfarra, U. Baltensperger, B. Buchmann, C. Hueglin, and A. S. H. Prevot (2007), Source apportionment of submicron organic aerosols at an urban site by factor analytical modelling of aerosol mass spectra, *Atmos. Chem. Phys.*, *7*, 1503–1522.

Liu, P., P. J. Ziemann, D. B. Kittelson, and P. H. McMurry (1995a), Generating particle beams of controlled dimensions and divergence: I. Theory of particle motion in aerodynamic lenses and nozzle expansions, *Aerosol Sci. Technol.*, *22*, 293–313.

Liu, P., P. J. Ziemann, D. B. Kittelson, and P. H. McMurry (1995b), Generating particle beams of controlled dimensions and divergence: II. Experimental evaluation of particle motion in aerodynamic lenses and nozzle expansions, *Aerosol Sci. Technol.*, *22*, 314–324.

Mao, H., and R. W. Talbot (2004), Relationship of surface O_3 to large-scale circulation patterns during two recent winters, *Geophys. Res. Lett.*, *31*, L06108, doi:10.1029/2003GL018860.

Marcolli, C., et al. (2006), Cluster analysis of the organic peaks in bulk mass spectra obtained during the 2002 New England Air Quality Study with an Aerodyne aerosol mass spectrometer, *Atmos. Chem. Phys.*, *6*, 5649–5666.

McLafferty, F. W., and F. Turecek (1993), *Interpretation of Mass Sectra*, University Science Books, Sausolito, CA.

Nemitz, E., J. L. Jimenez, J. A. Huffman, M. R. Canagaratna, D. R. Worsnop, and A. B. Guenther (2008), An eddy-covariance system for the measurement of surface/atmosphere exchange fluxes of submicron aerosol chemical species — First application above an urban area, *Aerosol Sci. Technol.*, in press.

O'Dowd, C. D., M. C. Facchini, F. Cavalli, D. Ceburnis, M. Mircea, S. Decesari, S. Fuzzi, Y. J. Yoon, and J.-P. Putaud (2004), Biogenically driven organic contribution to marine aerosol, *Nature*, *431*, 676–680.

Peltier, R. E., A. P. Sullivan, R. J. Weber, C. A. Brock, A. G. Wollny, J. S. Holloway, J. A. deGouw, and C. A. Warneke (2007), Fine aerosol bulk composition measured on the WP-3D research aircraft in vicinity of the Northeastern United States – Results from NEAQS, *Atmos. Chem. Phys.*, *7*, 3231–3247.

Pope, C. A., R. T. Burnett, M. J. Thun, E. E. Calle, D. Krewski, K. Ito, and G. D. Thurston (2002), Lung cancer, cardio-pulmonary mortality, and long-term exposure to fine particulate air pollution, *J. Am. Med. Assoc.*, *287*, 1132–1141.

Quinn, P. K., et al. (2006), Impacts of sources and aging on submicrometer aerosol properties in the marine boundary layer across the Gulf of Maine, *J. Geophys. Res.*, *111*, D23S26, doi:10.1029/2006JD007582.

Reid, J. S., R. Koppmann, T. F. Eck, and D. P. Eleuterio (2005), A review of biomass burning emissions Part II: Intensive physical properties of biomass burning particles, *Atmos. Chem. Phys.*, *5*, 799–825.

Rhupaketi, M., et al. (2005), An intensive study of the size and composition of submicron atmospheric aerosols at a rural site in Ontario, Canada, *Aerosol Sci. Technol.*, *39*, 722–736.

Roberts, J. M., F. C. Fehsenfeld, S. C. Liu, M. J. Bollinger, C. Han, D. L. Albritton, and R. E. Sievers (1984), Measurements of aromatic hydrocarbon ratios and NO_x concentrations in the rural troposphere: Estimates of air mass photochemical age and NO_x removal rate, *Atmos. Environ.*, *18*, 2421–2432.

Russell, L. M., A. A. Mensah, E. V. Fischer, B. C. Sive, R. K. Varner, W. C. Keene, J. Stutz, and A. A. P. Pszenny (2007), Nanoparticle growth following photochemical α- and β-pinene oxidation at Appledore Island during ICARTT/CHAiOS 2004, *J. Geophys. Res.*, *112*, D10S21, doi:10.1029/2006JD007736.

Salcedo, D., et al. (2007), Technical note: Use of a beam width probe in an aerosol mass spectrometer to monitor particle collection efficiency in the field, *Atmos. Chem. Phys.*, *7*, 549–556.

Schichtel, B. A., K. A. Gebhart, W. C. Malm, and M. G. Barna (2005), Reconciliation and interpretation of Big Bend National Park particulate sulfur source apportionment: Results from the Big Bend Regional Aerosol and Visibility Observational study - Part I, *J. Air Waste Manage. Assoc.*, *55*, 1709–1725.

Schneider, J., et al. (2004), Online mass spectrometric aerosol measurements during the MINOS campaign (Crete, August 2001), *Atmos. Chem. Phys.*, *4*, 65–80.

Schneider, J., S. Weimer, F. Drewnick, S. Borrmann, G. Helas, P. Gwaze, O. Schmid, M. O. Andreae, and U. Kirchner (2006), Mass spectrometric analysis and aerodynamic properties of various types of combustion-related aerosol particles, *Int. J. Mass Spectrom.*, *258*, 37–49.

Seinfeld, J. H. and S. N. Pandis (2006), *Atmospheric Chemistry and Physics From Air Pollution to Climate Change*, Wiley-Interscience, New York.

Shah, S. D., D. R. Cocker III, J. W. Miller, and J. M. Norbeck (2004), Emission rates of particulate matter and elemental and organic carbon from in-use diesel engines, *Environ. Sci. Technol.*, *38*, 2544–2550.

Sive, B. C., Y. Zhou, D. Troop, Y. L. Wang, W. C. Little, O. W. Wingenter, R. S. Russo, R. K. Varner, and R. W. Talbot (2005), Development of a cryogen-free concentration system for measurements of volatile organic compounds, *Anal. Chem.*, *77*, 6989–6998.

Sullivan, A. P., R. E. Peltier, C. A. Brock, J. A. deGouw, J. S. Holloway, C. Warneke, A. G. Wollney, and R. J. Weber (2006), Airborne measurements of carbonaceous aerosol soluble in water over northeastern United States: Method development and an investigation into water-soluble organic carbon sources, *J. Geophys. Res.*, *111*, D23546, doi:10.1029/2006JD007072.

Takami, A., T. Miyoshi, A. Shimono, and S. Hatakeyama (2005), Chemical composition of fine aerosol measured by AMS at Fukue Island, Japan during APEX period, *Atmos. Environ.*, *39*, 4913–4924.

Talbot, R. W., H. Mao, and B. C. Sive (2005), Diurnal characteristics of surface level O_3 and other important traces gases in New England, *J. Geophys. Res.*, *110*, D09307, doi:10.1029/2004JD005449.

Tsigaridis, K., and M. Kanakidou (2007), Secondary organic aerosol importance in the future atmosphere, *Atmos. Environ.*, *41*, 4682–4692.

Turpin, B. J., and J. J. Huntzicker (1991), Secondary formation of organic aerosol in the Los Angeles Basin: A descriptive analysis of organic and elemental carbon concentrations, *Atmos. Environ., Part A*, *25*, 207–215.

Turpin, B. J., and H. J. Lim (2001), Species contributions to $PM_{2.5}$ mass concentrations: revisiting common assumptions for estimating organic mass, *Aerosol Sci. Technol.*, *35*, 602–610.

United States Environmental Protection Agency (2001), Air quality criteria for particulate matter (second external review draft), *EPA Rep. EPA 600/P-99/002a,b,2v*, Office of Research and Development, Research Triangle Park, NC.

Volkamer, R., J. L. Jimenez, F. San Martini, K. Dzepina, Q. Zhang, D. Salcedo, L. T. Molina, D. R. Worsnop, and M. J. Molina (2006), Secondary organic aerosol formation from anthropogenic air pollution: Rapid and higher than expected, *Geophys. Res. Lett.*, *33*, L16804, doi:10.1029/2006GL026310.

Warneke, C., et al. (2004), Comparison of daytime and nighttime oxidation of biogenic and anthropogenic VOCs along the New England coast in summer during New England Air Quality Study 2002, *J. Geophys. Res.*, *109*, D10309, doi:10.1029/2003JD004424.

Warneke, C., et al. (2006), Biomass burning and anthropogenic sources of CO over New England in the summer of 2004, *J. Geophys. Res.*, *111*, D23S15, doi:10.1029/2005JD006878.

White, M. L., et al. (2008), Volatile organic compounds in northern New England marine and continental environments during the ICARTT 2004 campaign, *J. Geophys. Res.*, doi:10.1029/2007JD009161, in press.

Williams, B. J., et al. (2007), Chemical speciation of organic aerosol during ICARTT 2004: Results from in situ measurements, *J. Geophys. Res.*, *112*, D10S26, doi:10.1029/2006JD007601.

Zhang, Q., M. R. Canagaratna, J. T. Jayne, D. R. Worsnop, and J. L. Jimenez (2005a), Time and size-resolved chemical composition of submicron particles in Pittsburgh – Implications for aerosol sources and processes, *J. Geophys. Res.*, *110*, D07S09, doi:10.1029/2004JD004649.

Zhang, Q., D. R. Worsnop, M. R. Canagaratna, and J. L. Jimenez (2005b), Hydrocarbon-like and oxygenated organic aerosols in Pittsburgh: Insights into sources and processes of organic aerosols, *Atmos. Chem. Phys.*, *5*, 3289–3311.

Zhang, Q., M. R. Alfarra, D. R. Worsnop, J. D. Allan, H. Coe, M. R. Canagaratna, and J. L. Jimenez (2005c), Deconvolution and quantification of hydrocarbon-like and oxygenated organic aerosols based on aerosol mass spectrometry, *Environ. Sci. Technol.*, *39*, 4938–4952.

Zhang, Q., et al. (2006), Component analysis of organic aerosols in urban, rural, and remote atmospheres based on aerosol mass spectrometry, in *7th International Aerosol Conference*, St. Paul, Minnesota.

Zhang, Q., J. L. Jimenez, D. R. Worsnop, and M. R. Canagaratna (2007a), A case study of urban particle acidity and its effect on secondary organic aerosol, *Environ. Sci. Technol.*, *41*, 3213–3219.

Zhang, Q., et al. (2007b), Ubiquity and dominance of oxygenated species in organic aerosols in anthropogenically influenced northern hemisphere mid-latitudes, *Geophys. Res. Lett.*, *34*, L13801, doi:10.1029/2007GL029979.

Zhou, Y., R. K. Varner, R. S. Russo, O. W. Wingenter, K. B. Haase, R. W. Talbot, and B. C. Sive (2005), Coastal water source of short-lived halocarbons in New England, *J. Geophys. Res.*, *110*, D21302, doi:10.1029/2004JD005603.

Zhou, Y., H. Mao, R. Russo, D. R. Blake, O. W. Wingenter, K. Haase, J. Ambrose, R. K. Varner, R. Talbot, and B. Sive (2008), Bromoform and dibromomethane measurements in the seacoast region of New Hampshire, 2002–2004, *J. Geophys. Res.*, doi:10.1029/2007JD009103, in press.

Ziemba, L. D., E. V. Fischer, R. J. Griffin, and R. W. Talbot (2007), Aerosol acidity in northern New England: Temporal trends and source region analysis, *J. Geophys. Res.*, *112*, D10S22, doi:10.1029/2006JD007605.

P. J. Beckman, R. J. Griffin, B. C. Sive, R. W. Talbot, and L. D. Ziemba, Climate Change Research Center, University of New Hampshire, Durham, NH 03824, USA. (rob.griffin@unh.edu)

L. D. Cottrell, Environ, Groton, MA 01450, USA.

J. L. Jimenez and I. Ulbrich, Department of Chemistry and Biochemistry and Cooperative Institute for Research in the Environmental Sciences (CIRES), University of Colorado, Boulder, CO 80309, USA.

Q. Zhang, Atmospheric Sciences Research Center, State University of New York, University at Albany, Albany, NY 12203, USA.